OFFICE OF ENVIRONMENTAL HEALTH HAZARD ASSESSMENT

Air Toxics Hot Spots Program

Perchloroethylene Inhalation Cancer Unit Risk Factor

Technical Support Document for Cancer Potency Factors

Appendix B

September, 2016

Air, Community, and Environmental Research Branch
Office of Environmental Health Hazard Assessment
California Environmental Protection Agency

Page left intentionally blank

List of Acronyms

AIC	Akaike information criterion	MCL	Mononuclear cell leukemia
AUC	Area under the concentration curve	MCMC	Markov Chain Monte Carlo method
BMD	Benchmark Dose	mg-hr/(L-d)	Milligram-hours per liter per day
BMDL	Estimation of the BMD 95% lower	mg/kg-d	Milligram per kilogram per day
BMDS	Benchmark Dose Software	$\mu g/m^3$	Microgram per cubic meter
BW	Body weight	MLE	Maximum likelihood estimate
CDPH	California Department of Health Services	MOA	Mode of action
CYP450	Cytochrome P450	N-AcTCVC	N-acetyl-S-(1,2,2-trichlorovinyl)-cysteine
DCA	Dichloroacetic acid	NAT	N-acetyl transferase
DEHP	Diethyl hexyl phthalate	NCI	National Cancer Institute
DNA	Deoxyribose nucleic acid	NRC	National Research Council
DCVG	S-(1,2-dichlorovinyl)-glutathione	NTP	National Toxicology Program
FMO3	Flavin-containing mono-oxygenase 3	PBPK	Physiologically-based pharmacokinetic
GLP	Good Laboratory Practice standards	PCE	Perchloroethylene
GSH	Glutathione	PHG	Public Health Goal
GST	Glutathione-S-transferase	PPARα	Peroxisome proliferator-activated receptor-α
HEC	Human equivalent concentration	ppb	Parts per billion
IARC	International Agency for Research on Cancer	ppm	Parts per million
IRIS	Integrated risk information system (US EPA)	TAC	Toxic Air Contaminant
JBRC	Japan Bioassay Research Center	TCA	Trichloroacetic acid
JISHA	Japan Industrial Safety and Health Association	TCE	Trichloroethylene
LGLL	Large granular lymphocyte leukemia	TCVC	S-(trichlorovinyl)cysteine
		TCVG	S-(1,2,2-trichlorovinyl)-glutathione
		TSD	Technical Support Document
		URF	Unit risk factor
		US EPA	U.S. Environmental Protection Agency
		VOC	Volatile organic compound

PERCHLOROETHYLENE

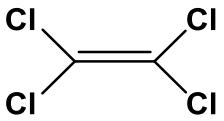

CAS Number: 127-18-4

1. INTRODUCTION

The Office of Environmental Health Hazard Assessment (OEHHA) develops potency values for carcinogenic substances that are candidate Toxic Air Contaminants (TACs) (Health and Safety Code Section 39660) or are listed under the Air Toxics Hot Spots Act (Health and Safety Code Section 44321). These values are used in the Air Resources Board's (ARB's) air toxics control programs and also by other State regulatory bodies, to estimate cancer risk in humans.

Perchloroethylene (PCE), also commonly referred to as tetrachloroethylene, was officially placed on the TAC list by the ARB in 1991. In support of that decision, the California Department of Health Services evaluated the toxicology of PCE and determined that it was a potential carcinogen in humans, besides displaying other forms of toxicity (CDHS, 1991). Shortly thereafter, OEHHA derived inhalation potency values for PCE using dose-response data from a National Toxicology Program (NTP) study of the chemical's carcinogenic effects in rodents (OEHHA, 1992; NTP, 1986). OEHHA's potency values were based upon the induction of liver tumors in male mice and incorporated a simple pharmacokinetic model to estimate internal metabolized doses.

The present document updates the dose-response analysis for inhalation exposure to PCE and derives a cancer unit risk factor (expressed as $(\mu g/m^3)^{-1}$) and corresponding cancer slope factor (expressed in $(mg/kg\text{-}d)^{-1}$) using OEHHA's current Air Toxics Hot Spots program risk assessment guidelines (OEHHA, 2009), as well as research made available since our last PCE review in 1992. In particular, OEHHA has identified an additional well-conducted, lifetime rodent inhalation study (JISHA, 1993); also, a refined physiologically-based pharmacokinetic (PBPK) model for PCE has been published (Chiu and Ginsberg, 2011). Both of these studies were used in the update. Where appropriate, the current analysis draws upon material from previous OEHHA evaluations, as well as recent toxicological assessments published by the US Environmental Protection Agency (US EPA, 2012a) and the International Agency for Research on Cancer (IARC, 2014).

2. SUMMARY OF DERIVED VALUES

OEHHA's revised potency values for PCE are based on the elevated incidence of several tumor types observed in male mice and rats in relation to PCE-metabolized doses calculated with a simplified adaptation of the Chiu and Ginsberg (2011) model. For dose-response calculations, OEHHA used US EPA's Benchmark Dose Software (BMDS) (US EPA, 2015) and its implementation of the multi-stage cancer model. BMDS was also

used to evaluate the multi-site tumor risks. After considering several issues related to data quality and analytical uncertainty, the geometric mean of 4 dose-response values was chosen as the best estimate of carcinogenic potency. The potency values for PCE, in terms of external exposure, are:

Unit Risk Factor $(\mu g/m^3)^{-1}$	6.1E-06
Slope Factor $(mg/kg\text{-}day)^{-1}$	2.1E-02

3. MAJOR SOURCES AND USES

PCE is a dense volatile liquid with an ether-like odor. It is used mainly as a chemical intermediate, solvent, and cleaning agent. The total US demand for PCE in 2004 was 355 million pounds (Dow, 2008). In the US, 60 percent of PCE use was for chemical production (e.g., to make hydrofluorocarbon alternatives to chlorofluorocarbons), 18 percent was used in surface preparation and cleaning, 18 percent in dry-cleaning and textile processing, and 4 percent for miscellaneous other uses (*ibid.*). Total air emissions of PCE in California for 2010 were estimated by ARB to be 3832 tons per year (ARB, 2012).

4. SELECTED PHYSICAL AND CHEMICAL PROPERTIES OF PCE

Molecular weight	165.83
Boiling point	121 ^oC
Melting point	-19 ^oC
Vapor pressure	18.47 mm Hg @ 25 ^oC
Air concentration conversion	1 ppm = 6.78 mg/m^3 @ 25 ^oC

(HSDB, 2010)

5. NATIONAL AND INTERNATIONAL HAZARD EVALUATIONS

According to the National Toxicology Program (NTP) 13th Report on Carcinogens (RoC), PCE is "reasonably anticipated to be a human carcinogen based on sufficient evidence of carcinogenicity from studies in experimental animals" (NTP, 2014). The RoC found that PCE exposure produced tumors in multiple tissue types of both sexes of mice and rats. For inhalation exposure, the tumor types cited by NTP were: mononuclear-cell leukemia in rats, tubular-cell kidney tumors in male rats and liver tumors in mice. Additionally, NTP noted increased liver tumors in mice exposed to PCE by ingestion.

IARC found that PCE is "probably carcinogenic to humans," citing limited epidemiological findings (primarily increased bladder cancer in dry cleaning workers) and sufficient evidence in experimental animals (IARC, 2014). For rodents, in addition to the tumor types listed by NTP, IARC notes an increased incidence of: hemangioma and hemangiosarcoma of the liver in mice, spleen and Harderian gland tumors in male mice,

brain and testicular tumors in male rats, and skin tumors in mice dermally exposed to the PCE metabolite, tetrachloroethylene oxide.

US EPA states that PCE is “likely to be carcinogenic in humans by all routes of exposure,” based upon suggestive epidemiologic data (bladder cancer, non-Hodgkin’s lymphoma, and multiple myeloma) and conclusive evidence from carcinogenicity studies in rodents (referring to the same set of tumors as above) (US EPA, 2012b).

PCE has been listed on California’s Proposition 65 list since 1988 as a chemical "known to the state to cause cancer." California’s Public Health Goal for drinking water is based on PCE-induced carcinogenicity (OEHHA, 2001).

6. TOXICOKINETICS

PCE is readily absorbed through the lungs and gastrointestinal tract, and can also be absorbed to a lesser extent through the skin. The blood-air partition coefficients of PCE in humans and rodents are in the range of about 15 to 20 (Chiu and Ginsberg, 2011). These values indicate the ratio by which the PCE concentration in blood will be greater than its concentration in air at equilibrium. Humans breathing air containing 100 ppm PCE over 8 hours absorbed approximately 70 percent of inhaled PCE after the first hour, and 50 percent of the PCE intake at the end of the exposure period (Fernandez, *et al.*, 1976). Once in the body, PCE disperses into all tissues, concentrating preferentially in fatty tissues. For example, in rats inhaling 500 ppm PCE for 2 hours, the area under the concentration curve (AUC) after 72 hours, in milligram-minutes per milliliter of tissue, was: 1493 (fat), 33 (brain), 31 (liver), 26 (kidney), and 8.4 (blood) (Dallas, *et al.*, 1994).

PCE has a relatively low rate of metabolism in rodents and humans and is primarily eliminated unchanged via exhalation. In rats exposed to 150 ppm PCE in drinking water for 12 hours and monitored for an additional 72 hours, approximately 88% of the body burden was eliminated unmetabolized by exhalation (Frantz and Watanabe, 1983). Ohtsuki, *et al.* (1983) monitored occupationally exposed dry-cleaning workers and estimated that at the end of an 8-hour exposure to 50 ppm, about 38% of absorbed PCE was exhaled unchanged and 2% metabolized and excreted in urine.

PCE Metabolites

The metabolism of perchloroethylene has been studied mostly in mice, rats, and humans. Detailed reviews of this literature have been published (Lash and Parker, 2001; Anders *et al.*, 1988; Dekant, 1986). Briefly, rodent studies have identified the following urinary metabolites:

- trichloroacetic acid (TCA)
- N-trichloroacetyl aminoethanol
- oxalic acid
- N-oxalylaminoethanol
- dichloroacetic acid (DCA)

- S-(1,2,2-trichlorovinyl)glutathione (TCVG)
- N-acetyl-S-(1,2,2-trichlorovinyl)cysteine (N-AcTCVC)

Trichloroacetic acid and N-AcTCVC have also been observed in the urine of exposed humans. The aminoethanol derivatives, N-trichloroacetyl aminoethanol and oxalyl aminoethanol, are thought to arise from the reaction of the intermediate acyl chlorides with phosphatidyl ethanolamine present in biological membranes (Dekant, *et al.*, 1986). Carbon dioxide has also been found as an exhaled metabolite. Trichloroethanol has been detected in urine samples in some studies, but not in others, and it is unclear whether it was produced from co-exposure to trichloroethylene (in occupational exposures), or in other cases, if it was an artifact of the analytical methods employed (Lash and Parker, 2001). More recent work (e.g., Yoshioka, *et al.*, 2002) has not detected trichloroethanol and supports the conclusion that it is not a significant PCE metabolite (US EPA, 2012a).

Metabolic Pathways

A simplified metabolic scheme for PCE is presented in Figure 1. Two main pathways of metabolism have been identified. The first, referred to here as the "oxidative pathway," involves initial oxidation of PCE by Cytochrome P450 (CYP450) enzymes. The second "GST pathway" is initiated by glutathione-S-transferase (GST)-catalyzed conjugation of PCE with glutathione (GSH).

In the oxidative pathway the primary CYP450 isoform involved is thought to be CYP2E1, based upon analogy with other small halogenated molecules, with additional participation of isoforms 2B1/2, and 3A (Lash and Parker, 2001). The main, chemically stable metabolic product of oxidation is trichloroacetic acid (TCA), formed by hydrolysis of the reactive intermediate trichloroacetyl chloride, the latter of which appears to be formed by molecular rearrangement of the substrate-CYP450 complex (Guyton, *et al.*, 2014). A secondary product is the reactive tetrachloroethylene oxide (PCE epoxide), which decomposes to oxalyl chloride and then to carbon monoxide and carbon dioxide (Yoshioka, *et al.*, 2002). Oxalic acid may also form from decomposition of PCE epoxide or directly from the substrate-enzyme complex (Guyton *et al.*, 2014).

The liver is considered the main site of metabolism for the oxidative pathway, although other tissues with appropriate CYP450 activity, e.g., lung, kidney, brain, and lymphocytes,[1] may oxidize PCE to a smaller extent.

The initial step in the GST pathway produces the conjugate, S-(trichlorovinyl)glutathione (TCVG). The tripeptide glutathione moiety of TCVG can then be degraded via enzymatic cleavage of its glycine and glutamine units, producing S-(trichlorovinyl)-cysteine (TCVC). TCVC may be subsequently transformed as follows:

[1] Lymphocyte microsomes from male Wistar rats have been found to contain CYP450 2B, 2E, and 3A activity at 20, 4, and 2.4 percent of liver microsomal activity. Lymphocyte CYP450 content can also be chemically induced, resulting in 2 to 4-fold increases in activity (Hannon-Fletcher and Barnett, 2008).

Figure 1: Simplified Metabolic Scheme for PCE [(a)]

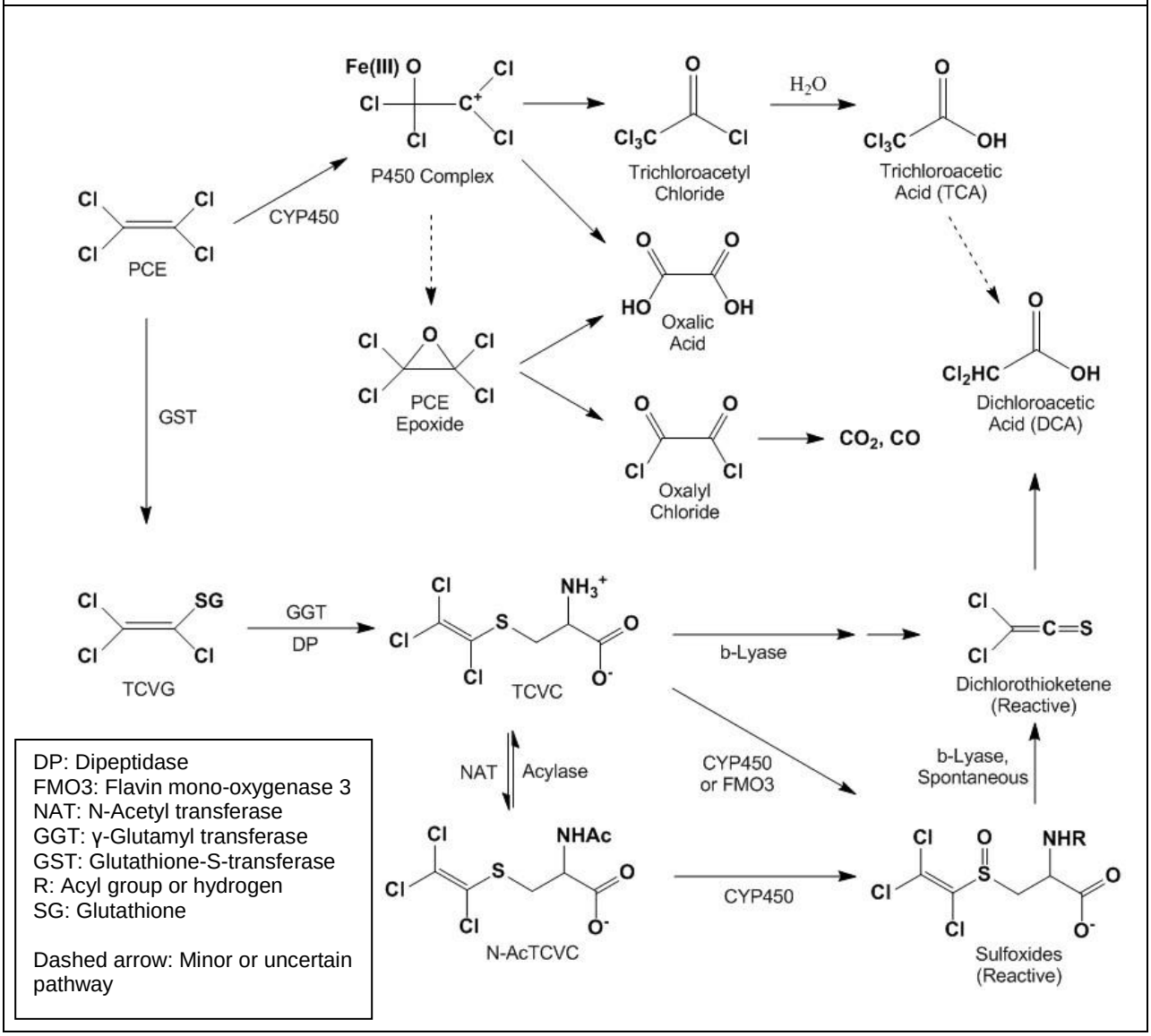

(a) From Guyton *et al.* (2014), US EPA (2012a), and Lash and Parker (2001).

- The free amino group of TCVC may be acylated by N-acetyl transferase, forming N-acetyl-S-(trichlorovinyl)cysteine (N-AcTCVC) which passes into urine; this process may also be reversed by acylases, regenerating TCVC.
- The sulfur atom of TCVC and N-AcTCVC may be oxidized by CYP450 or flavin-containing mono-oxygenase 3 (FMO3); this process forms reactive α,β-unsaturated sulfoxides that can bond with nucleophilic biological molecules or spontaneously decompose to dichlorothioketene, itself a reactive metabolite.
- The carbon-sulfur bond of TCVC may be cleaved by β-lyase, releasing an unstable trichlorovinyl thiol that spontaneously decomposes to dichlorothioketene.

Dichloroacetic acid, believed to arise mainly by hydrolysis of dichlorothioketene, was found in rat but not human urine. Evidence for this mechanism comes from the detection of a covalent protein adduct, N-(dichloroacetyl)-L-lysine, in rat kidney cells (Birner *et al.*, 1994).

Multi-Organ Metabolism in the GST Pathway

The GST pathway involves a series of enzymatic transformations with cycling of metabolic intermediates mainly between the liver and kidney, and including some entero-hepatic processing. The initial glutathione conjugation step occurs primarily in the liver, forming TCVG which is transported to the blood and bile. The kidney epithelium actively absorbs the circulating conjugate from blood for further processing and excretion. As noted above, this involves cleavage of TCVG by gamma glutamyl transferase (GGT) and dipeptidase (DP) to form TCVC. The amino group of TCVC can then be acylated to form mercapturate N-AcTCVC in the kidney, or TCVC may recirculate back to the liver for acylation (Lash and Parker, 2001).

In some species, such as rabbit and guinea pig, significant intrahepatic processing of glutathione conjugates may occur, with formation of TCVC from TCVG by the bile-duct epithelium, followed by reabsorption into hepatocytes and subsequent acylation. Additionally, TCVG excreted via the bile can be converted to TCVC in the intestinal lumen and undergo entero-hepatic cycling (Hinchman and Ballatori, 1994; Irving and Elfarra, 2013).

The kidney is viewed as the main site for formation of genotoxic metabolites by β-lyase cleavage of TCVC since β-lyase activity is relatively high in this organ. Smaller amounts of β-lyase have been found in other organs, such as the liver, brain, and spleen (Rooseboom, *et al.*, 2002), raising the possibility that reactive dichlorothioketene may be generated and produce genetic damage in other tissues independent of its production in the kidney. Although the liver contains a form of β-lyase, enzymatic cleavage of TCVC does not appear to be toxicologically significant in this organ. For example, in rats treated with the PCE-conjugate analogues, dichlorovinyl glutathione (DCVG) and dichlorovinyl cysteine (DCVC), significant pathology was observed in the kidney, but no tissue damage was seen in the liver (Lash and Parker, 2001).

Oxidation of TCVC and N-AcTCVC to the reactive α,β-unsaturated sulfoxides can occur in the liver and kidney, as well as other organs that contain flavin mono-oxygenase 3 (FMO3) or CYP450 3A activity. As noted above, the sulfoxides are reactive Michael acceptors and can bond with nucleophilic sites on biological molecules. Discussing the metabolism of trichloroethylene (TCE), Irving and Elfarra (2012) noted that the α,β-unsaturated sulfoxides formed in the GST pathway may be further conjugated with glutathione, but that this process could also be reversible (by retro-Michael addition). This would create a mechanism by which the reactive sulfoxides could circulate in a stabilized form through the blood to other organs where they may be regenerated. The mechanism would likely be operative for PCE as well.

Pharmacokinetic Model

Numerous physiologically based pharmacokinetic (PBPK) models have been proposed for PCE over the course of several decades. Reddy (2005), Clewell (2005), and US EPA (2012a) have reviewed this body of research. Although the models are reasonably consistent in estimating PCE blood concentrations, they differ widely in their predictions of metabolized PCE at lower exposure concentrations. For example, at an inhaled concentration of 1 ppb, some models predict about 1 or 2 percent metabolism, while others predict metabolism in the range of 20 to 35 percent, and perhaps as high as 60 percent (Chiu and Ginsberg, 2011). Since PCE's carcinogenic potency is likely to depend upon the formation of genotoxic metabolic products, the wide range of estimated PCE metabolism among models has been a recognized problem for assessing the cancer risk from low-level PCE exposure.

The most recent and comprehensive PBPK model for PCE is that of Chiu and Ginsberg (2011). It was developed following the recommendations of the National Research Council (NRC, 2010) that the available models for PCE be integrated into a single harmonized model incorporating various improvements. The Chiu and Ginsberg (2011) model incorporates lung, liver, kidney, fat, and venous blood compartments, and lumped compartments for rapidly and slowly perfused tissues. It has components for simulating inhalation, oral, and injection exposures.[2] Absorption-desorption of PCE in the upper respiratory tract (i.e., the "wash-in/wash-out" effect) is also taken into account. The rate of PCE oxidation is modeled in liver, kidney and lung, and GSH conjugation is modeled in the liver and kidney. The model can estimate (for example): concentrations of PCE in exhaled air, blood concentrations of PCE and TCA, and urinary excretion of TCA and the GSH-conjugation metabolites, N-AcTCVC and DCA. A graphical representation of the Chiu and Ginsberg PBPK model is provided in Figure 2.

US EPA (2012a) used the Chiu and Ginsberg (2011) model to estimate internal dose metrics in its recent PCE cancer potency factor update, which included the development of a URF for inhalation exposures. The most important improvements of the Chiu and Ginsberg (2011) model, as discussed by the US EPA (2012a), are:

- It uses Bayesian Markov Chain Monte Carlo (MCMC) methodology to determine the most likely values (posterior modes) for key metabolic constants.
- The model considered all the available toxicokinetic data for PCE in mice, rats, and humans, and is calibrated using a wide range of *in vivo* toxicokinetic data.
- It is the first model to include a separate glutathione conjugation pathway.
- It incorporates recent information on TCA toxicokinetics from trichloroethylene modeling studies.

[2] Note that the Chiu and Ginsberg model does not include dermal absorption of PCE vapor, which is considered to be relatively small in rodents and humans. For example, McDougal et al. (1990) measured dermal absorption in rats exposed to 12,500 ppm PCE vapor and found that dermal uptake was about 3.5% of inhalation + dermal uptake. Percutaneous penetration of PCE vapor in humans exposed to 600 ppm was approximately 1% of pulmonary absorption (Riihimaki and Pfaffli, 1978).

Figure 2: Chiu and Ginsberg (2011) PBPK Model for PCE [(a)]

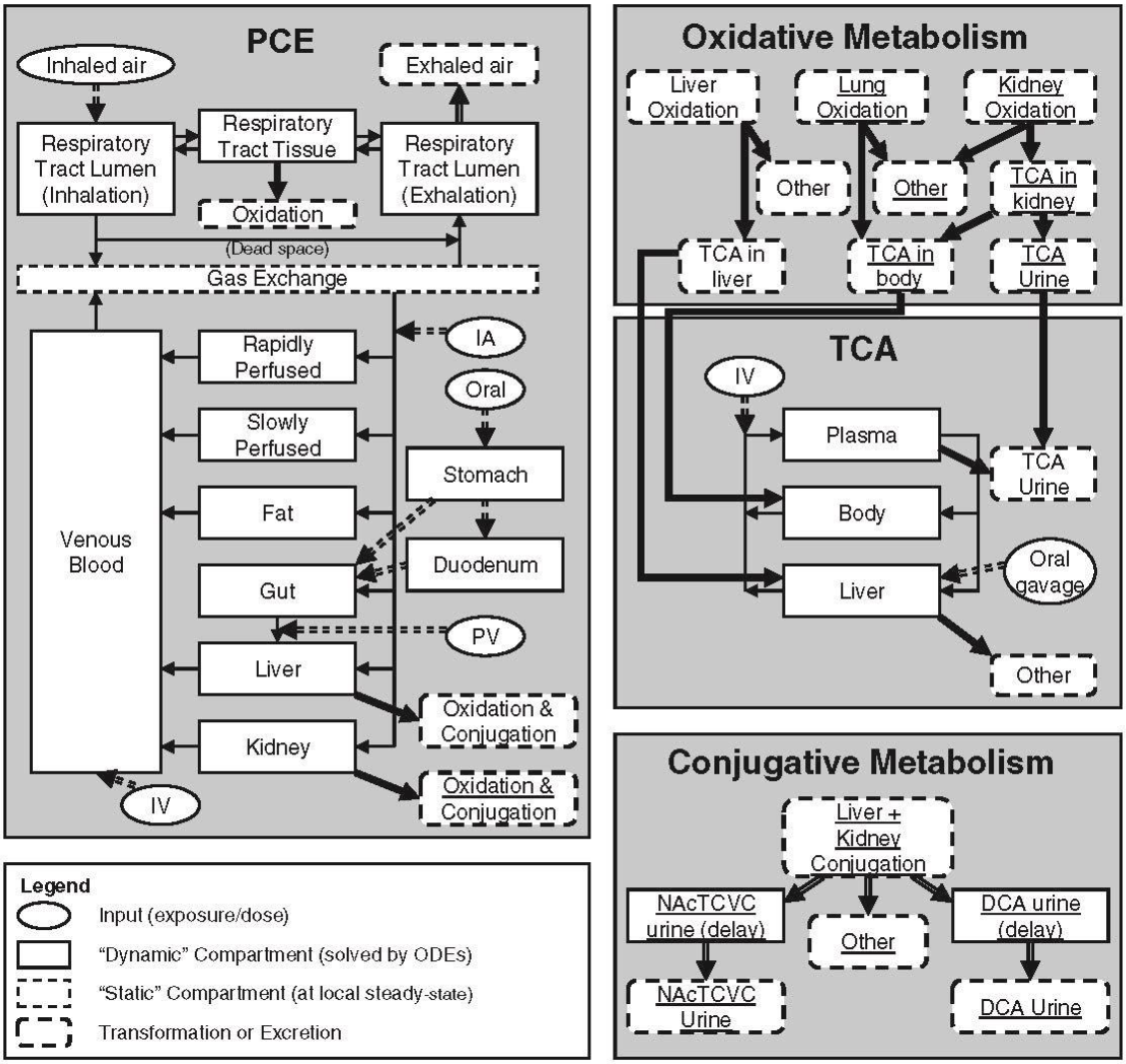

(a) Figure adapted from Chiu and Ginsberg (2011). IV = intravenous, IA = intra-arterial, PV = portal vein.

Chiu and Ginsberg (2011) used a hierarchical Bayesian population approach to obtain estimates of the posterior modes[3] for a subset of important PBPK model parameters including: the pulmonary ventilation rate, metabolic constants for oxidation and conjugation of PCE, and urinary excretion of metabolites. Other model parameters, such as partition coefficients and most of the physiological parameters, were fixed at baseline values chosen from the literature. Inclusion of several intake routes (e.g., inhalation, oral, and intravenous) allowed the model to be calibrated and evaluated against a wide variety of experimental *in vivo* data.

[3] These are also the maximum likelihood estimates (MLEs) since flat prior distributions were used in the model.

In the MCMC analysis, sampling variation was characterized by running multiple chains of length 5000 (retaining every 10th value) using randomly chosen starting conditions for each chain. For the rodent PBPK models, 24 independent MCMC chains were run, each producing a chain-specific, posterior mode estimate. The parameter set with highest overall posterior probability of all the chains was selected as the posterior mode of the optimized PBPK model. For the human model, 48 independent chains were used since preliminary analysis indicated a potential for multiple maxima.

Table 1 shows a summary of predictions for several types of dose metrics based on the optimized model for inhalation exposures, reported by Chiu and Ginsberg (2011). With respect to the PCE AUC and PCE oxidation metrics, the range of chain-specific values was less than 40% of the overall posterior mode estimates. For example, in the mouse model at 1 ppm exposure, the overall posterior mode for percent of PCE oxidized was 17.4% of intake, and the range of chain-specific posterior modes was 11.5% to 17.9%.[4]

The estimates for PCE conjugation were more variable (with the exception of the rat model). In mice exposed at 1 ppm, for example, the model predicts that 0.016% of PCE intake will be conjugated with a range of 0.0068% to 0.43%. In the human model, the overall posterior mode indicates that 9.4% of PCE intake is metabolized by GSH conjugation, with a range of 0.003% to 10%. The human model displayed an apparent bimodal distribution for the rate of GSH conjugation. Nonetheless, the most probable posterior mode was at the high end of estimated conjugation rates. Regarding the results for humans, Chiu and Ginsberg (2011) note that:

> "The parameter optimization procedure revealed two distinct modes in the rate of GSH conjugation — one with 'high' GSH conjugation (the overall posterior mode) and one with 'low' GSH conjugation (a number of the alternative posterior modes). The log-likelihood for the overall posterior mode with high GSH conjugation is 38 units higher than the alternative posterior modes with low GSH conjugation, which would be significant by any classical statistical test."

Chiu and Ginsberg (2011) were not able to determine how much of the spread in the human conjugation model was due to uncertainty or population variation, but pointed out that the distribution could represent actual variability given the large differences in GST activities displayed by humans. On the other hand, a high level of variability was not observed in metabolic studies of trichloroethylene (TCE). Lash *et al.* (1999) looked at rates of GSH conjugation of TCE in 40 ethnically and age-diverse, male and female human liver samples and found less than a 10-fold variation.

As noted above, US EPA (2012a) used Chiu and Ginsberg's model results to derive its updated PCE potency factors. However, because of the large range of model estimates for PCE conjugation, US EPA prioritized the dose metrics based on oxidative metabolism and PCE AUC in their final analysis.

[4] Ranges of MCMC chain-specific posterior modes are from Table S-8 of Chiu and Ginsberg, 2011.

Table 1: PCE Internal Dose Metrics from the Chiu and Ginsberg (2011) PBPK Model (and reproduced by the OEHHA model extract) [(a)]

Constant Inhalation Doses (posterior mode estimates)

Dose metric	Exposure Concentration (ppm)					Prediction Range (at 1 ppm)
	0.01	***1***	***10***	***100***	***1000***	
PCE AUC Blood	*(mg-hr)/(L-d) per ppm*					
Mouse	2.1	2.2	2.4	2.6	2.7	2.2-2.4
Rat	2.25	2.25	2.25	2.25	2.4	2.25-2.27
Human	2.0	2.0	2.0	2.0	2.0	2.0-2.4
PCE Oxidation	*Percent of intake that is oxidized*					
Mouse	18.8	17.4	11.8	7.3	6.6	11.5-17.9
Rat	4.2	4.2	4.1	3.3	1.1	3.9-4.2
Human	0.98	0.98	0.98	0.98	0.98	0.69-1.0
PCE Conjugation	*Percent of intake that is conjugated*					
Mouse	0.015	0.016	0.021	0.025	0.026	0.0068-0.43
Rat	0.31	0.31	0.31	0.32	0.335	0.20-0.50
Human [(b)]	9.4	9.4	9.4	9.4	9.3	0.003-10.0 (bimodal)[(b)]

(a) Values are from Chiu and Ginsberg (2011), Tables S-6 through S-8, and are also reproduced by OEHHA's inhalation-only model extract, at the presented level of significance.
(b) Values presented are for the most probable posterior mode.

Use of Chiu and Ginsberg (2011) Harmonized PBPK Model

Although there are unresolved issues related to the Chiu and Ginsberg model predictions for PCE's GST pathway, OEHHA considers the model to be the best available methodology for estimating dose metrics in the dose-response assessment. Regarding uncertainty in GSH conjugation, the Office evaluated the effect of including the GST pathway in the dose metric on the overall cancer potency analysis (see the following section).

The full Chiu and Ginsberg (2011) model contains large portions of code designed to perform the Bayesian MCMC simulation, which determined the posterior mode estimates for key PBPK parameters. Once obtained, the posterior modes can be used to forecast the most likely values for internal doses at various exposure concentrations.

For the inhalation potency evaluation, OEHHA relied on Chiu and Ginsberg's optimized PBPK model results. Since only dose metrics for inhalation exposures needed to be

estimated, the inhalation-relevant portion of the Chiu and Ginsberg (2011) model was extracted. Specifically, OEHHA: (1) identified the main inhalation components of the MC-Sim program obtained from the authors, (2) extracted the relevant equations and inputs from the model code and translated them from the MC-Sim language into Berkeley Madonna code, (3) ran the code using the optimized, Bayesian posterior mode parameters and other baseline values developed by Chiu and Ginsberg (2011), and (4) tested the output against the original model dose estimates reported in the Chiu and Ginsberg (2011) paper.

A graphic depicting OEHHA's inhalation-only model is presented in Figure 3. As in the original Chiu and Ginsberg model, it includes lung, liver, kidney, fat, and venous blood compartments, and lumped compartments for rapidly and slowly perfused tissues. The first transformation in the oxidative pathway is modeled in the lung, liver, and kidney, and the first step of the GST pathway is included for liver and kidney. Absorption-desorption of PCE in the upper respiratory tract is also included. The model adequately reproduced the predictions of the original Chiu and Ginsberg model for inhalation exposures: OEHHA's model extract reproduces the internal dose-metric values obtained by Chiu and Ginsberg (2011), as presented in Table 1.[5] The Berkeley Madonna model code for mouse, rat, and human is provided in Appendix A.

Uncertainty and/or Variation in the Model Estimates

Additional discussion of the uncertainty related to GSH conjugation, particularly in the human model, is provided here to support the choice of dose metric (presented later, in Section 9). Four issues are addressed as follows.

First, as noted above, the modeled rate of GSH conjugation in humans displayed a relatively high amount of uncertainty and/or variation: 0.003 -10%, with the overall posterior mode at 9.4% of intake. Commenting on this large range, Chiu and Ginsberg (2011) noted that the *in vivo* data available for model calibration were "inadequate to constrain the flux through this pathway, either extreme providing plausible fits to the data."

The overall posterior mode for PCE conjugation is, however, consistent with the *in vitro* rates for TCE and other halogenated VOCs that have been reported in the literature (e.g., Lash *et al.*, 1998; and Wheeler, *et al.*, 2001). The low value for PCE conjugation is consistent with the low-end of *in vitro* activity obtained for PCE by Dekant *et al.* (1998), which were below the analytical method detection limits.[6]

[5] OEHHA's model extract reproduced the dose-metric estimates reported in Tables S-6 through S-8 of the original Chiu and Ginsberg (2011) paper, typically to 3 significant figures.

[6] It should be noted that the *in vitro* GSH-conjugation data was not used to calibrate the model.

Figure 3: Inhalation-Only PBPK Model for PCE [(a)]

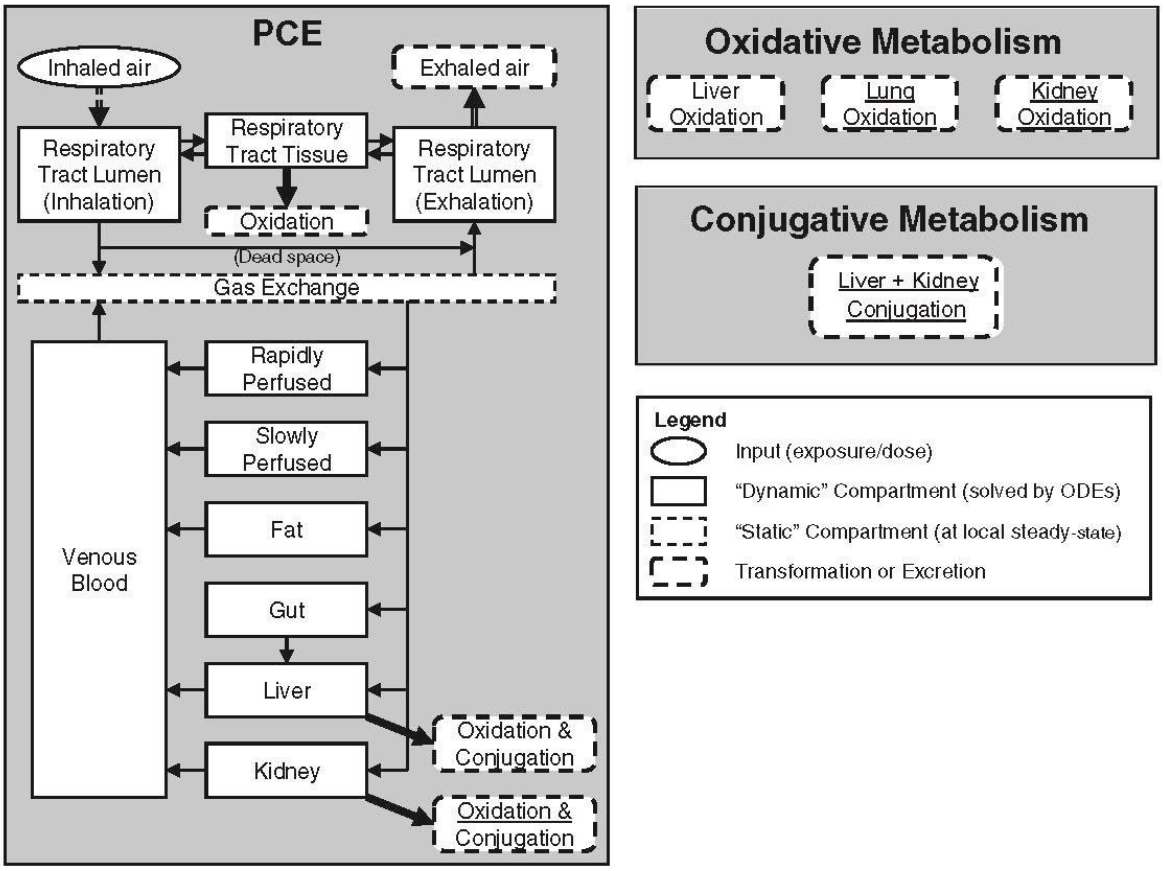

(a) Figure adapted from Chiu and Ginsberg (2011).

The large prediction range obtained in the human conjugation model raises a question - particularly with regard to interspecies dose extrapolation - of whether the model's GSH conjugation estimates should be used along with the PCE oxidation rates in a "total metabolized dose" metric. The alternative would be to define an internal dose metric using only the less-variable model predictions for PCE oxidation, as was done by US EPA (2012a).[7]

The impact of PBPK model uncertainty in this case is muted when both PCE oxidation and GSH conjugation are included together as a total metabolized dose, increasing the potency estimate by about one order of magnitude (much less than the range observed in the MCMC analysis).

[7] Omitting GSH-conjugation from the internal dose metric is similar to using the lower-likelihood mode for human GSH-conjugation in a total metabolized dose. With the lower mode, the rates of conjugation for humans, rats, and mice would all be small relative to PCE oxidation rates, and thus have little impact on both the dose-response calculations using the rodent data and interspecies dose extrapolation using the human PBPK model.

In order to demonstrate this, OEHHA compared the results of interspecies dose extrapolation using the human PBPK model with the two alternative dose metrics, i.e., using either total metabolism (GSH-conjugation + PCE oxidation) or PCE oxidation-only metabolism. We used the model to calculate human equivalent concentrations (HECs) from a range of example benchmark doses that could be obtained from the dose-response modeling of PCE exposure in rodents. As can be seen from the PBPK-derived HEC values presented in Table 2, the total metabolism dose metric produces HECs that are about 11-fold smaller than HECs obtained using an oxidation-only dose metric (Note that smaller HECs result in larger cancer potency factors).

Table 2: Impact of Internal Dose Metric Choice on Interspecies Conversion Calculations

Example Benchmark Doses [(a)] (mg/kg-d)	PBPK-Derived Human Equivalent Concentration (HEC; ppm)		Ratio of HECs
	Oxidative + GSH Conjugation	Oxidative Metabolism Only	
0.1	0.61	6.5	10.7
1.0	6.1	65.0	
3.0	18.2	195.0	

(a) Since oxidative metabolism is significantly greater than GSH conjugation in rodents, both dose metrics will produce similar benchmark doses in the rodent dose-response models. A rough HEC comparison can therefore be made on a single benchmark dose for both dose-metric scenarios.

Thus, it appears that using a dose-metric incorporating a "high-end" value for human GSH conjugation, as opposed to using an oxidation-only dose metric which effectively sets GSH-conjugation to zero, adds a relatively small amount of "conservatism" to the dose-response analysis. OEHHA has determined that inclusion of the GST pathway in a total metabolized dose metric ensures that the resulting potency values are adequate to protect public health, per the recommendations of our current Air Toxics Hotspots program risk assessment guidelines (OEHHA, 2009).

A second issue is whether using the model's uncertain estimate for glutathione conjugation in mice could have a large impact upon the dose-response calculation. As above, this question is addressed by looking at the difference between using either total metabolism or oxidation-only metabolism as the dose metric. In this case, the impact would be low. From Table 1, the model's posterior mode estimates of PCE oxidation and conjugation in mice indicate that oxidation dominates conjugation by factors of 290-1250, such that both dose metrics (total and oxidation-only) reflect mainly PCE oxidation, and should produce similar benchmark doses in a dose-response model.

Third, there is an unresolved disagreement regarding the large variation in the results of key *in vitro* studies that have estimated glutathione conjugation of PCE and TCE in rodent and human tissues. In its IRIS PCE review, the US EPA (2012a) pointed out:

> "The GSH pathway for tetrachloroethylene was originally demonstrated only in rodents, and interpretation of the then-existing data led some scientists to conclude that the pathway was not operative in humans (Green *et al.*, 1990). More recent data clearly demonstrate the existence of the pathway in humans (Schreiber *et al.*, 2002; Völkel *et al.*, 1998; Birner *et al.*, 1996) [...]
>
> "There are discrepancies regarding reported rates of tetrachloroethylene GSH metabolism (Lash *et al.*, 2007; Lash and Parker, 2001; Dekant *et al.*, 1998; Lash *et al.*, 1998; Green *et al.*, 1990). These differences may be due, in part, to different chemical assay methodology or to problems resulting from the stability of the chemical product being measured or both (Lash and Parker, 2001)."

Some of the *in vitro* studies predict relatively high TCVG (and DCVG) production rates in humans (e.g., Lash *et al.*, 1998; Lash *et al.*, 1999), while others indicate very low conjugation. For example, with TCE, Green *et al.* (1997) measured DCVG formation at 0.19 picomole per minute per milligram protein (pmol/min/mg) using human liver cytosol from 4 individuals. Conversely, Lash *et al.* (1999) measured TCE conjugation at 5,770 (pmol/min/mg) in human cytosolic protein pooled from 20 individuals. This large difference in measured GSH conjugation rates is reflected in the uncertainty/variability displayed by the Chiu and Ginsberg human model (and to a lesser extent, the mouse model).

Several commentators have raised doubts regarding the accuracy of the PCE and TCE conjugation rates reported by Lash *et al.* (1998, 1999, 2007), pointing to potential issues with the chemical analysis methods used by the laboratory. On the other hand, the apparent chemical instability of the GSH conjugates raises questions for studies that have measured low conjugate levels. However, no work has apparently been done to determine the true source of the discrepancy among the various divergent study results. The Lash laboratory has published several papers following Lash *et al.* (1998) involving the analysis of TCVG and DCVG, and has described various quality controls used ensure analytical accuracy.[8] Consistent results were generally obtained in these studies. On the other hand, Lash, *et al.* (2006) measured DCVG levels in blood and tissue samples of rats orally exposed to TCE and obtained a mixture of high and unexpectedly low values. However, the higher values obtained by Lash *et al.* (2006) were generally consistent with blood DCVG concentrations found in orally exposed mice by Kim *et al.* (2009), and with mouse tissue and serum concentrations measured by Yoo, *et al.* (2015), both using a different method of analysis.

Discrepancies in measured conjugation rates in humans might also be due to variable quality of the tissue samples used, and it is possible that some samples were not representative of the known variation in human GST activities. Thus, OEHHA does not

[8] For example, see Lash *et al.* (2007) and Lash, *et al.* (1999).

find convincing evidence to discount the high-end *in vitro* values for human glutathione conjugation of PCE, and estimated by the Chiu and Ginsberg (2011) PBPK model as well.

Finally, as Chiu and Ginsberg (2011) noted, a large part of the spread in estimated human conjugation rates may be due to biologic variation in the human population. Three important classes of GST enzyme have been identified in human liver cytosol: GSTA, GSTM, and GSTT. Both GSTM and GSTT have isoforms, GSTM-1 and GSTT-1, that are absent in a relatively large fraction of the population as a result of genetic variation (in this case due to gene deletion). Moyer *et al.* (2007) investigated the prevalence of GSTM-1 and GSTT-1 null individuals in the population and found frequencies of 50.5 - 78%, and 33.5 - 73.5%, respectively. Ginsberg *et al.* (2009) reported that some ethnic groups have high percentages of members that are null in both the GSTM-1 and GSTT-1 isoforms. For example, more than 30% of ethnic Chinese people appear to lack both enzymes.

It is currently not known which GSTs are most active in conjugating PCE. However, it appears that some low molecular weight halogenated hydrocarbons, such as dichloromethane, are primarily conjugated by GSTT-1. If PCE is a substrate mainly of GSTT-1 or GSTM-1, then the presence of many individuals lacking these enzymes would produce a large range of variability in the rate of PCE conjugation.

7. GENOTOXICITY AND CARCINOGENICITY

Genotoxicity

A large number of studies have tested the genotoxicity of PCE, and less frequently its metabolites, in microorganisms, mammalian cells, and in *Drosophila* and rodents. There have also been a few occupational exposure studies looking at genetic abnormalities in lymphocytes. This literature has recently been reviewed in detail by IARC (2014) and US EPA (2012a). Selected results based on these reviews and the literature are presented below.

PCE was not mutagenic in the Ames test with *S. typhimurium* or *E. coli* in the presence or absence of S9 metabolic activation. It was mutagenic, however, in *S. typhimurium* when tested with purified rat-liver GST, glutathione, and rat kidney fractions, where TCVG would be formed (Vamvakas, *et al.*, 1989). Most studies looking at chromosomal aberrations, micronuclei formation, or sister chromatid exchange have been negative, but micronuclei induction was seen in Chinese hamster ovary cells (Wang *et al.*, 2001) and human lymphoblastoid cells expressing CYP450 enzymes (White *et al.*, 2001). Genetic alterations have also been observed in rapidly growing yeast cell cultures (US EPA, 2012a).

Other types of tests, such as DNA strand break assays, DNA-adduct and cell transformation studies, and *Drosophila* mutation tests have provided mixed results. Positive findings include: Elevated DNA single-strand breaks in mouse liver and kidney *in vivo* (Walles, 1986), and DNA-adduct formation in mouse and rat tissues *in vivo* (Mazzullo, *et al.*, 1987).

Results from occupational studies have also been mixed. Ikeda *et al.* (1980) tested ten factory workers exposed to high (92 ppm PCE) or low (10-40 ppm) and found no evidence of cytogenetic damage to lymphocytes or altered cell cycle kinetics. No increase in sister chromatid exchanges in lymphocytes was found in a study of 27 subjects exposed to 10 ppm (geometric mean) of PCE (Seiji *et al.*, 1990). A decrease (not increase) of 8-hydroxy-deoxyguanosine, a marker of oxidative DNA damage, was observed in leukocytes of 38 female dry cleaners exposed to average concentrations of less than 5 ppm PCE (Toraason *et al.*, 2003). On the other hand, a study of 18 dry-cleaning workers exposed to 3.8 ppm PCE (average) found evidence of short-term genetic damage to peripheral blood lymphocytes, indicated by an increase in acentric chromosomal fragments (Tucker *et al.*, 2011).

Genotoxicity testing of various PCE metabolites includes the following positive results:

- TCA exhibited genotoxicity in several *in vivo* tests, for example: DNA strand breaks, chromosomal abnormalities, and micronucleus formation in mice; and chromosomal aberrations in chicken bone marrow (IARC, 2014; US EPA, 2012a).
- Genotoxicity has been demonstrated with DCA in the Ames test, micronucleus induction test, a mouse lymphoma assay, and *in vivo* cytogenetic tests; DCA has also been shown to cause DNA strand breaks *in vivo* in mouse and rat liver (*ibid.*).
- Trichloroacetyl chloride vapor tested positive in the Ames test with and without metabolic activation (DeMarini, *et al.*, 1994).
- PCE epoxide was mutagenic without metabolic activation in the Ames test with *S. typhimurium* TA1535 at the lower doses tested; toxicity occurred at higher doses (Kline *et al.*, 1982).
- TCVG incubated with rat kidney protein containing γ-glutamyl transpeptidase (GGT) and dipeptidases was mutagenic in the Ames test (Vamvakas, *et al.*, 1989).
- TCVC and N-AcTCVC tested positive in the Ames test without metabolic activation (Dekant *et al.*, 1986; Vamvakas, *et al.*, 1987).
- TCVC sulfoxide was mutagenic in the Ames test with *S. typhimurium* TA 100, but was 30-fold less potent than TCVC (Irving and Elfarra, 2013).

The GST-pathway metabolites, TCVG and TCVC, appear to be relatively potent mutagens based upon the available genotoxicity data (Lash and Parker, 2001).

In addition, several metabolites have been tested for carcinogenicity in animals. Dermal exposure of mice to PCE epoxide induced skin tumors (Van Duuren, *et al.,* 1983). Several long-term drinking-water bioassays of TCA and DCA in mice, with limited pathologic analysis of tissues other than the liver, found increases in hepatocellular tumors. Initiation–promotion studies with TCA or DCA in mice also demonstrated that

they promote liver tumors following initiation by other carcinogens (IARC, 2014; Guyton *et al.*, 2014).

Cancer Epidemiology

Numerous epidemiologic studies of PCE have been published, including more than 25 larger cohort and case-control studies since OEHHA's last toxicity review (*circa* 2000, for our PHG for drinking water). Several detailed reviews of the literature have recently been published (Guyton, *et al.*, 2014; IARC, 2014; and US EPA, 2012a).

Epidemiologic studies of PCE have all relied on semi-quantitative measures of exposure such as high/medium/low, ever/never exposed, or job categories. As such, the exposure data in this body of research are not of sufficient quality for use in quantitative dose-response analysis. However, it provides evidence that PCE causes cancer in humans and qualitatively supports the development of a unit risk value from animal studies. US EPA (2012a) evaluated the results of the cohort and case-control studies that developed more precise exposure assessments and concluded that PCE increases the risk of three types of cancer in humans: bladder cancer, non-Hodgkin's lymphoma (NHL), and multiple myeloma. IARC (2014) agreed with US EPA regarding bladder cancer, but concluded that the evidence for PCE inducing other cancers in humans was insufficient given the conflicting results across various studies. With non-Hodgkin's lymphoma, for example, "three cohort studies showed an increased risk based on small numbers, and the largest study with the best control of potential confounders did not. Case-control studies on non-Hodgkin lymphoma did not find significant associations" (*ibid.*).

A recent meta-analysis of bladder cancer risk in dry-cleaning workers (Vlaanderen, *et al.*, 2014) integrated the results of seven studies and 139 exposed cases, and found an overall relative risk level of about 1.5 for exposed versus non-exposed groups (with a 95% confidence level of 1.16 to 1.85).

Animal Studies of PCE

Increased tumor incidence was found in mice and rats in three long-term carcinogenicity studies of PCE. An oral study was conducted by the National Cancer Institute (NCI,1977), where $B6C3F_1$ mice and Osborne-Mendel rats were administered PCE in corn oil by gavage, 5 days/week for 78 weeks with additional follow-up of 32 weeks for rats and 12 weeks for mice. PCE caused a significant increase of hepatocellular carcinomas in mice of both sexes, and the tumors appeared considerably sooner in treated mice than in controls. Survival in the high dose groups was much lower than the control group at 40 to 45 weeks, and toxic nephropathy was observed in 93% of mice exposed. In rats, a high level of early mortality occurred in all treated groups, which obscured conclusions regarding carcinogenicity.

Two lifetime inhalation bioassays of PCE have also been published and are described as follows.

A lifetime inhalation cancer study was conducted by the Japan Bioassay Research Center (JBRC) of the Japan Industrial Safety and Health Association (JISHA, 1993). Good Laboratory Practice (GLP) standards were used in the conduct of the study. Dose-response data was analyzed by standard statistical procedures and study results were thoroughly documented in a manner similar to NTP rodent cancer study reports.

The study was conducted using F344/DuCrj rats and Crj:BDF_1 mice. Groups of 50 male and 50 female rats were exposed to PCE (99.0% pure) at 50, 200 or 600 ppm, and similar groups of mice were exposed to 10, 50, or 250 ppm, for 6 hours per day, 5 days per week, and 104 weeks. During the study period, the general status, body weight, and food consumption of the animals were monitored. Urinalyses, hematological, and blood chemistry tests were performed near the end of exposure for the surviving animals. Upon death, animals were necropsied and organ weights were determined. Histopathologic examination of all major tissue types was performed on all animals. Survival was good for both sexes of rats and mice in all dose categories: more than 80 percent of rats and 70 percent of mice were alive at week 92. Nonetheless, survival was significantly reduced at the highest exposure levels when compared with control groups.

Additional findings related to tumorigenesis are (see also Table 3):

- For exposed male and female rats, the only tumor type that was found to be elevated was mononuclear cell leukemia (MCL). A statistically significant dose-response trend was found by the Cochran-Armitage and exact trend tests (in males) or a life-table test (in females). In addition, for males, the highest dose category displayed a significant increase when compared to controls by the Fisher exact test.

- In exposed mice, an increased incidence of hepatocellular adenoma and carcinoma was found in both sexes as indicated by significant dose-response trends and pair-wise comparison of the high dose category against controls. In the males, there was also an increase in all-organ, hemangioma or hemangiosarcoma (mostly in the spleen and liver), and Harderian gland tumors.

NTP (1986) conducted a study where B6C3F1 mice and F344/N rats, in groups of 50, were exposed to PCE (99.9% pure) by inhalation, 6 hours/day, 5 days/week for 103 weeks. Mice were exposed to concentrations of 100 or 200 ppm, and rats to 200 or 400 ppm, in addition to controls. The general status and body weight of the animals were monitored during the study. Upon death, animals were necropsied and histopathologic examination of all relevant tissues was performed on all animals. Approximately 70 percent or more of both sexes of mice and rats were alive at week 90 of the study. Survival was significantly reduced in male rats at the higher exposure level when compared with controls. Survival was decreased in both dose levels in male mice and in the high dose group of female mice.

As shown in Table 4, PCE significantly increased the rate of hepatocellular carcinomas in mice of both sexes. The combined incidence of liver adenoma or carcinoma was also

increased, although the incidence of liver adenomas separately was not. In female and male rats, PCE also produced significant increases in mononuclear cell leukemia (MCL). Male rats additionally exhibited apparent increases in tumor incidence in the kidney, brain, and testes. Statistical tests for increases in renal tubular-cell adenomas and adenocarcinomas appeared to be dose-related, but did not reach customary significance levels. However, the historical incidence of these tumors is low (0.4%) at the laboratory and increased incidence has been found with other chlorinated ethanes and ethylenes. Thus renal tubular-cell tumors were judged to be related to PCE exposure. Brain glioma, another rare tumor type in F344 rats, was observed in one male control rat and in four male rats at 400 ppm exposure. This increase was not statistically significant. However, because the historical incidence of these tumors is 0.8% for the laboratory, the increased brain tumor incidence in this study was also carried though the analysis. Testicular interstitial cell tumors showed significant dose-responses in both life table and incidental tumor tests calculated by NTP. This tumor type was therefore included in the dose-response evaluation, but was considered to be more uncertain, given the high background rate of testicular tumors in F344 rats (both historically and in the NTP study controls)

Primary Studies for the Dose-Response Assessment

Both the NTP (1986) and JISHA (1993) inhalation studies were judged to be of high quality and suitable for the development of an inhalation potency factor. The studies used different strains of mice (Crj:BDF_1 vs. B6C3F_1) and different substrains of F344 rats. They displayed variability of outcome with respect to the tissues affected, as well as the strength of the dose-response relationships for various tumor types, and differing incidence rates in the control groups. Some of this variability could be due, in the case of the rat models, to the fact that the different substrains used may have genetic and phenotypic variation as a result of mechanisms such as genetic drift.

For example, Tiruppathi *et al.* (1990) and Thompson *et al.* (1991) reported that the Japanese and German substrains of the Fischer 344 (F344) rat, but not the US substrain, were deficient in dipeptidyl dipeptidase-4 activity in the kidney and liver. This enzyme has been implicated in the degradation of collagen, blood clotting, immunomodulation, and metabolism of hormonal peptides (Tiruppathi, *et al.*, 1990). While this particular enzymatic variation may not be directly relevant to PCE metabolism, it indicates that F344 rat substrains can display significantly divergent biological traits. With regard to the mice, the genetic variation issue is accentuated by the use of two different mouse hybrid strains, not substrains.

Table 3: Primary Tumor Incidence in Mice and Rats Exposed to PCE Rates at Exposure Concentrations in PPM (JISHA, 1993)

Mice (Crj:BDF$_1$)

Tumor Type	Sex	Adjusted Rates[(a)(b)] (at 0-250 ppm)				Rate Percent (at 0-250 ppm)			
		0	10	50	250	0	10	50	250
Hepatocellular adenoma or carcinoma	M	13/46**	21/47	19/47	40/49**	28.3	44.7	40.4	81.6
	F	3/44**	3/41	7/40	33/46**	6.8	7.3	17.5	71.7
Hemangioma or hemangiosarcoma (All sites)	M	4/46*	2/47	7/47	9/49*	8.7	4.3	14.9	18.4
Harderian gland adenoma	M	2/41**	2/45	2/37	8/39	4.9	4.4	5.4	20.5

Rats (F344/DuCrj)

Tumor Type	Sex	Adjusted Rates[(a)(b)] (at 0-600 ppm)				Rate Percent (at 0-600 ppm)			
		0	50	200	600	0	50	200	600
Mononuclear cell leukemia	M	11/50**	14/48	22/50	27/49*	22.0	29.2	44.0	55.1
	F	10/50[(c)]	17/50	16/50	19/50	20.0	34.0	32.0	38.0

(a) Tumor-incidence denominator adjusted by excluding animals dying before the first corresponding tumor type observed in each study.

(b) Statistical test indicators: (*) P-value < 0.05; (**) P-value < 0.005. Fisher exact test results are as reported by JISHA, except that mouse, all-site hemangioma/hemangiosarcoma values were calculated by OEHHA. The control group column indicates the results of trend tests. Both the Cochran-Armitage trend test (reported by JISHA) and the exact trend test calculated by OEHHA gave the same indications of significance.

(c) A significant trend was found in a life-table test reported by JISHA, P-value = 0.049.

Table 4: Primary Tumor Incidence in Mice and Rats Exposed to PCE Rates at Exposure Concentrations in PPM (NTP, 1986)

Mice ($B6C3F_1$)

Tumor Type	Sex	Adjusted Rates[a][b] (at 0-200 ppm)			Rate Percent (at 0-200 ppm)		
		0	100	200	0	100	200
Hepatocellular adenoma or carcinoma	M	17/49**	31/47**	41/50**	34.7	70.0	82.0
	F	4/44**	17/42**	38/47**	9.1	40.5	80.9

Rats (F344/N)

Tumor Type	Sex	Adjusted Rates[a][b] (at 0-400 ppm)			Rate Percent (at 0-400 ppm)		
		0	200	400	0	200	400
Mononuclear cell leukemia	M	28/50*	37/48*	37/50*	56.0	77.1	74.0
	F	18/49*	30/50*	29/50*	36.1	60.0	58.0
Renal tubule adenoma or carcinoma	M	1/47[c]	3/42	4/40	2.1	7.1	10.0
Brain glioma	M	1/44[c]	0/37	4/35	2.3	0.0	11.4
Testicular interstitial cell	M	35/49[c]	39/46	41/50	71.4	84.8	82.0

(a) Tumor-incidence denominator adjusted by excluding animals dying before the first corresponding tumor type observed in each study.

(b) Statistical test indicators: (*) P-value < 0.05; (**) P-value < 0.005. Fisher exact test results are as reported by NTP. The control group column indicates the results of trend tests. Both the Cochran-Armitage trend test (reported by NTP) and the exact trend test calculated by OEHHA gave the same indications of significance.

(c) Although testicular tumors and brain glioma did not appear to be significantly increased by the Fisher exact and trend tests, life table tests conducted by NTP did show significant increases in trends of <0.001, and 0.039 respectively. In addition, NTP's incidental tumor tests showed increased testicular tumors by both trend and pair-wise comparisons. The life table trend test for kidney tumors was nearly significant at 0.054.

Although it cannot be determined whether the different outcomes for mice and rats observed by NTP (1986) and JISHA (1993) resulted from differences in animal biology, the data suggest that each study provides non-redundant information for the analysis.

The JISHA dataset offers the advantage of an additional dose category for each species, as well as the use of several lower exposure concentrations. Moreover, the control rate of MCL incidence in the F344/DuCrj rats used in the Japanese study (22 and 20%) was significantly lower than for the F344/N rats used in the NTP study (56 and 36%), and is expected to improve the precision of the fitted model. The NTP study, nonetheless, provides important additional data on tumor development in the kidney, brain, and testes of F344/N rats, and supporting data on the dose-response rate for MCL.

Based on the above considerations, OEHHA chose both the JISHA (1993) and NTP (1986) bioassays as primary studies for the dose-response analysis. The dose-response data and results of statistical tests are presented in Tables 3 and 4. Given the availability of two acceptable inhalation studies, the oral NCI (1977) study was not used in the quantitative analysis.

Relevance of MCL to Humans

Some concerns about the propriety of using the rat MCL data for human risk assessment were raised by an NRC expert panel (without consensus) during a review of US EPA's PCE IRIS evaluation (NRC 2010). One issue brought up by the panel was that MCL is a common tumor in aging F344 rats that lacks a corresponding tumor in humans. Panel members also questioned the statistical significance of the MCL dose-response data in light of the elevated historical and control-group incidence rates for MCL. This section briefly addresses both questions.

Regarding the issue of tumor-site concordance, current research in cancer biology indicates that the basic cellular mechanisms of carcinogenesis are similar among mammals. However, this does not imply that exposure to a chemical carcinogen will always produce cancer in the same organ in different species (US EPA, 2005). In the case of human leukemias and lymphomas that are known to be induced by specific carcinogens, rodents develop different types of leukemia and lymphoma (US EPA, 2012c). The sites of induced cancer may not be the same because of differing toxicokinetics and tissue susceptibilities. For leukemia and lymphoma, variation in susceptibility could be related to differences in hematopoiesis and immune surveillance. Accordingly, there is no expectation—in general or specifically for MCL—of tumor-site concordance when using animal studies to predict human cancer risk (OEHHA, 2009).

Notwithstanding this general principle, there is evidence that rat MCL corresponds to at least one form of human leukemia. The specific cell type and biological mechanisms that give rise to rat MCL are not known, but it appears to arise from a lymphocyte or monocyte lineage, and it is thought that the cell of origin resides in the spleen or undergoes neoplastic transformation in the spleen (Thomas *et al.*, 2007). One reasonable hypothesis is that rat MCL is a form of Large Granular Lymphocyte Leukemia (LGLL), a cancer that develops in the spleen and is phenotypically and functionally similar to human LGLL (IARC, 1990; Thomas *et al.*, 2007). Human LGLL derives from either T-cell or natural killer (NK) cell lineages (Sokol and Loughran, 2006). Additional support for linking rat MCL to

human LGLL is provided by a study using the F344 rat MCL as a model for human NK-LGLL, which observed similar cellular responses in samples of the two tumor-cell types (Liao *et al.*, 2011).

Exposure of humans and animals to relatively low doses of PCE produces adverse effects upon blood and the immune system (e.g., see: Marth, 1987; Kroneld, 1987; and Emara *et al.*, 2010) that could plausibly give rise to a variety of carcinogenic response in different species. In addition to human LGLL, rat MCL may correspond to other types of human leukemia or lymphoma.

Regarding statistical issues arising from the elevated incidence of MCL in control groups, an NTP workshop focusing on the high background incidences of MCL and other tumors in the F344 rat noted that, “From a statistical perspective, high background rates of such tumors in control animals will generally decrease the ability to detect an exposure-related effect. In addition, when a statistically significant tumor effect is found in test animals relative to concurrent controls, the effect may not be considered exposure-related if it falls within the range observed in historical controls” (King-Herbert and Thayer, 2006). The foregoing statement focuses on the problem of false negative test results. However, since US EPA found MCL incidence to be significantly elevated in PCE-exposed rats, NRC panel members were concerned with the potential for false positive test results. On this issue, OEHHA agrees with the Massachusetts Department of Environmental Protection (MDEP), who reviewed the historical background rates of MCL in the NTP and JISHA study laboratories and found that,

> "For both the NTP (1986) and JISHA (1993) studies, the background rate of MCL in the same study control group was greater than or equivalent to the historical control rates for the same lab, same sex. Thus, the controls in both studies did not exhibit anomalously low MCL, which could, had it occurred, lead to false positive responses in the treatment groups." (MDEP, 2014)

Indeed, for the JISHA male rat MCL data, where the incidence in study controls was 22%, the historical incidence was 6-22%, and the Cochran-Armitage test for trend was highly significant, having a p-value of less than 0.0005.

8. MODE(S) OF ACTION

PCE's carcinogenic modes of action (MOA) likely involve the genotoxicity of one or more of its oxidative- or GST-pathway metabolites, although the precise mechanisms are unknown.

Several PCE metabolites, e.g., PCE epoxide, oxalyl chloride, trichloroacetyl chloride, dichlorothioketene, and the TCVC sulfoxides, are reactive compounds and expected to have short half-lives in the nucleophile-rich cellular environment.[9] These substances will tend to react chemically and enzymatically with cellular components near their site of production. The relatively stable metabolites, such as: TCA, DCA, TCVC, and N-AcTCVC, are more likely to circulate throughout the body where they may be further metabolized

[9] For example, the high reactivity of PCE epoxide is indicated by its 2.6-minute half-life in a neutral aqueous buffer solution at 37° C (Yoshioka, *et al.*, 2002).

and impact tissues other than the liver and kidney.

Both trichloroacetic acid (TCA) and dichloroacetic acid (DCA) have independently been found to increase tumor formation in mice. Since TCA is a major metabolite of PCE, US EPA (2012a) evaluated whether it could be the primary source of PCE's carcinogenicity in mouse liver. Using dose-response data from the JISHA (1993) and NTP (1986) PCE studies and a drinking water study of TCA in mice (DeAngelo, *et al.*, 2008), US EPA found that metabolically-generated TCA could contribute from 12 to 100 percent of the increased risk of liver tumors. This large range is not highly informative, and leaves open the possibility that other reactive metabolites may contribute significantly to the production of liver tumors in mice.

There are several non-genotoxic MOAs that may contribute to PCE's carcinogenicity, though in as yet poorly understood ways. These have been discussed at length by US EPA (2012a), and include: cytotoxicity with subsequent cellular proliferation, oxidative stress-induced cellular transformation, and dysregulation due to altered DNA methylation. Two specific MOAs that are potentially relevant for evaluating PCE involve α2u-globulin nephropathy in the male rat, and PPARα activation[10] for mouse liver tumors. In both cases, the biological bases for these MOAs in rodents are thought to be muted or absent in humans, indicating that the particular tumor-types may not be useful for human risk assessment.

α2u-Globulin Nephropathy

The α2u-globulin MOA in male rats is defined by: accumulation of α2u-globulin-containing hyaline droplets in the proximal tubules of the kidney, cytotoxicity with tubular cell proliferation, exfoliation of epithelial cells into the proximal tubular lumen and formation of granular casts, papillary mineralization, hyperplastic foci, and renal tumors (US EPA, 1991).

Green *et al.* (1990) found accumulation of α2u-globulin in the proximal tubules of F344 rats exposed by inhalation to 1000 ppm of PCE for 10 days, or given 1500 mg/kg PCE by gavage for 42 days. However a 400 ppm inhalation exposure for 28 days did not produce protein droplets or other signs of toxicity. For chemicals known to cause α2u-globulin toxicity, the formation of protein droplets in the kidney occurs rapidly upon exposure (frequently after a single dose), and further indications of tissue damage begin to appear in 3 to 4 weeks (Lehman-McKeeman, 2010; Green *et al.*, 1990). Thus, the absence of α2u-globulin accumulation after a 28-day exposure suggests that 400 ppm of PCE will not result in α2u-globulin toxicity upon long-term exposures.

The NTP (1986) study provided additional evidence along these lines. Karyomegaly and cytomegaly were observed in the kidneys of rats exposed to 200 or 400 ppm for 2 years, but indicators of α2u-globulin nephropathy (e.g., hyaline droplets, mineralization, and cast formation) were not found. The NTP protocol at the time was not designed to detect hyaline droplets or α2u-globulin accumulation (US EPA 2012a) but would have observed other markers of α2u-globulin toxicity if this MOA had been in effect. Moreover, comparable toxicity was observed in female rats in the NTP study, and PCE caused

[10] PPARα = "peroxisome proliferator-activated receptor-α."

similar kidney damage in rats and mice of both sexes in the NCI (1977) gavage study. This suggests that PCE's nephrotoxicity is neither sex nor species specific, as would be expected with an α2u-globulin MOA.

PPARα Activation

The PPARα MOA involves activation of the PPARα nuclear receptor, which is hypothesized to cause alterations in cell proliferation and apoptosis, and clonal expansion of initiated cells. The proposed indicators for this mode of action are: (1) PPARα activation with associated peroxisome proliferation, or (2) PPARα-activation plus increased liver weight and effects such as increased peroxisomal β-oxidation, CYP4A, or acyl CoA oxidase (Klaunig, *et al.*, 2003).

Numerous studies have been carried out to verify the PPARα MOA. The evidence obtained from this body of research has been mixed, and it currently remains unclear whether this hypothetical MOA is a major causal factor in mouse-liver tumor formation. The US EPA has published several detailed reviews of the PPARα MOA in its IRIS program toxicity reviews for PCE and TCA (US EPA 2012a, 2011). The main conclusions of these reviews are:

- PPARα activators can produce multiple effects in addition to peroxisome proliferation, including genotoxicity, oxidative stress, hypomethylation of DNA, and activation of other nuclear receptors.
- Peroxisome proliferation and the associated markers of PPARα activation are poor predictors of hepatocarcinogenesis in mice and rats. Studies with various PPARα activators show that the correlation between *in vitro* PPARα activation potency and tumorigenesis is weak and this relationship does not appear to be due to differences in pharmacokinetics. This suggests the involvement of carcinogenic mechanisms other than PPARα-activation.
- Studies of the PPARα-agonist, diethyl hexyl phthalate (DEHP) in transgenic mouse strains, although not fully conclusive, have cast doubt on whether the key events in the PPARα MOA (receptor activation, hepatocellular proliferation, and clonal expansion) are sufficient to cause liver tumors. The studies suggest that DEHP can induce tumors in a PPARα-independent manner (Ito *et al.*, 2007a), and that PPARα activation in hepatocytes is insufficient to cause tumorigenesis (Yang *et al.*, 2007). This again indicates that other mechanisms, either independently or in combination with PPARα-activation, are necessary to induce tumors.
- PCE exposure leads to PPARα-activation and modest levels of peroxisome proliferation, predominantly through its metabolite TCA. There is conflicting evidence as to whether this causes cellular proliferation in animals exposed to PCE: the peroxisome proliferation caused by PCE lacks specificity and consistency with respect to tissue, species, dose, and sequence of events. Also, there is little evidence indicating that PCE can induce clonal expansion of initiated cells. The available information for PCE is insufficient to demonstrate that the PPARα MOA plays a significant causative role in mouse hepatocarcinogenesis.

Conclusion on PCE's Mode(s) of Action

Given the limited understanding of the various non-genotoxic MOAs that may modify or add to the tumorigenic effects of PCE's genotoxic metabolites, there are insufficient grounds to evaluate PCE as primarily a non-genotoxic carcinogen using a non-linear model.

9. DOSE-RESPONSE ASSESSMENT

Dose Metrics

Much of the following information has already been presented, but is briefly restated here because of its relevance to choosing metrics for the dose-response calculations:

- The liver is the main site of oxidative PCE-metabolite formation, but other tissues with CYP 450 2E1, 2B, and 3A activity may also contribute to the oxidative-pathway. TCA is a relatively stable metabolite that has been found to increase liver tumors in mice via oral exposure. TCA's cancer potency in other tissues has not been adequately examined.
- Of the two metabolic pathways, oxidation is the main pathway in rodents. For example, at 10 ppm exposure, the PBPK model indicates that the ratio of oxidation to glutathione conjugation is 600 in mice and 19.5 in rats.
- Saturation of the oxidative pathway begins to occur between 1 and 10 ppm exposure in mice, and between 10 and 100 ppm exposure in rats (see Table 1). Saturation causes the ratio of oxidized to absorbed PCE to decrease at higher exposure concentrations. The smaller amount of metabolism that occurs via the GST pathway, on the contrary, increases somewhat at higher exposure concentrations in rodents.
- Although most GST conjugation of PCE takes place in the liver, the kidney is likely to be the main site for production of reactive GST-pathway metabolite dichlorothioketene. Other metabolites such as: TCVC, N-AcTCVC, and TCVC sulfoxide are formed in both the liver and kidney, and may circulate to other metabolizing tissues as well.
- It is not known which PCE metabolites, or even which of the two main metabolic pathways produces the most carcinogenic risk. However, genotoxicity tests suggest that some GST-pathway metabolites are relatively potent genotoxicants.
- The PBPK model for the GST pathway in humans involves a large variability or uncertainty, with two possible values (posterior modes) for the rate of PCE conjugation that differ by a factor of approximately 3000. However, as was discussed earlier in Section 6, the impact of the human PBPK model uncertainty/variability upon the overall dose-response evaluation is several orders of magnitude lower than this. It is not known how much of the model variability is due to the wide range of GST activities that have been observed in the human population, but it is reasonable to assume that some segment of the population could be efficient metabolizers while other segments (e.g., individuals who are homozygous in GST-null variants) could be much less efficient. It is currently unclear which GST isoforms are most active with regard to PCE conjugation.

- The more probable and larger of the two values indicates that glutathione conjugation predominates over oxidation in humans, the ratio of PCE conjugation to oxidation being about 10.

OEHHA considered the advantages and disadvantages of using several dose metrics for the dose-response calculations. These are briefly discussed below.

- Applied air concentration: This would be the simplest approach in that it does not rely upon the output of complicated PBPK modeling calculations. However, given the large body of evidence indicating that PCE's metabolites are likely to be responsible for its tumorigenic properties, using applied concentration as the dose metric may reduce the accuracy of the dose-response analysis, especially for the mouse, where the dose-response data indicate significant metabolic saturation in the oxidative pathway at the higher PCE exposure concentrations tested.

- PCE blood concentration: This dose metric does make use of the PBPK modeling estimates but has the same weakness as using the applied air concentration, since blood concentrations of the parent compound may not be directly related to concentrations of the potentially carcinogenic metabolites of PCE. Blood concentrations of PCE may even be less accurate than applied concentrations, since PCE blood concentrations are expected be inversely related to metabolite concentrations (For example, see Table 1 entries for the mouse dose-metrics where "PCE AUC per ppm exposure" increases and "percent oxidation/ppm" decreases) as one moves to higher exposure concentrations).

- Pathway specific metabolized dose: Defining a dose metric based upon either the oxidation or GST conjugation pathway would be better in terms of focusing on the production of PCE's carcinogenic metabolites instead of the parent compound. However, using either of the two pathways alone would be problematic, since each pathway produces several genotoxic substances that could be important for PCE's overall tumorigenicity. From Table 1 it can be seen that for mice, the quantity of oxidative metabolites produced with increasing exposure appears to be inversely related to the quantity of conjugation metabolites. Furthermore, if humans are more efficient conjugators than rodents, using an oxidation-only dose metric could underestimate the dose-response function. On the other hand, using glutathione conjugation alone has the problem of large model uncertainties with larger impacts upon the overall dose-response assessment (note that this impact is muted for total metabolism, as discussed above in Section 6).

- Choosing one or more metabolites: Using a subset of concentrations of one or more metabolites for the dose metric has similar problems as using pathway specific metabolism. For example, in Section 8 we briefly discussed US EPA's evaluation of TCA, a major metabolite generated in the oxidation pathway, where it was estimated that TCA might be responsible for as little as 12 percent of liver tumor risk in mice. An added issue is that the available PBPK models only incorporate a few of the various metabolites, such as TCA and DCA.

- Total PCE metabolized dose: Using total metabolism for the dose metric accounts for toxicokinetic differences across species and provides a dose adjustment for saturation effects in the oxidative pathway. It has the advantage of taking into account both pathways generating potentially carcinogenic metabolites. However, it involves assuming that carcinogenic potency is proportional to the combined rate of the first step of metabolism in each pathway. This assumption is simplistic but unavoidable given the many unknowns involved in PCE's toxicokinetics and toxicodynamics. As noted above, total metabolized dose has an advantage over using either oxidative or glutathione conjugation alone. Using oxidation-only may not be adequately protective of human health given the potential genotoxicity of metabolites formed in the conjugation pathway. Total metabolized dose is also advantageous compared with using the GST-pathway metabolites alone, since the PBPK modeling uncertainties have relatively little impact upon the dose-response assessment using total metabolism as the metric.

Considering all of the above factors, total metabolism (using the high-end, and more health-protective model estimate for GST conjugation in humans) was chosen as the best dose metric for the dose-response analysis of all the tumor types identified in the primary mouse and rat studies.[11] The PBPK-estimated, total metabolized doses used in the dose-response analysis are presented in Appendix B.

Dose-Response Model

Based upon its metabolic profile and the genotoxic activity of some of the metabolites formed, OEHHA considers PCE to be a genotoxic carcinogen. This information supports the assumption that the dose-response relationship approaches linearity at low doses and the use of the multistage cancer model to estimate the potency factor. This is consistent with OEHHA risk assessment guidelines, which indicate that use of the multistage model (and assuming low-dose linearity) is reasonable under such circumstances (OEHHA, 2009). In the traditional, linearized-multistage model, cancer potency is estimated as the upper 95% confidence bound, (q_1*), on the linear coefficient (q_1) in the following expression relating lifetime probability of cancer (p) to dose (d):

$$p = q_0 + (1 - q_0)\left(1 - exp\left[-\left(q_1 d + q_2 d^2 + \cdots\right)\right]\right)$$

In the above equation, (*d*) represents the average daily dose resulting from a uniform, continuous exposure over the nominal lifetime of the animal (two years for both mice and rats); (q_0) is the tumor incidence in the non-exposed group. For studies where the exposures vary in time, they are averaged over the entire study period and modeled as if they were uniform and continuous. Prior to fitting the dose-response model to the study data, an adjustment is made to the incidence rates to account for inter-current mortality, which decreases the pool of animals at risk of developing tumors throughout the study.

The latest version of BMDS (Version 2.6.0.1, US EPA, 2015) was used to carry out the

[11] In using total metabolized dose as the preferred dose metric, OEHHA considered the uncertainty in the available scientific information and, in contrast to US EPA (2012a), has chosen a modeling approach that will produce a more health-protective potency estimate. This is consistent with OEHHA's cancer risk assessment guidelines (OEHHA 2009), which establish a policy of developing cancer potency factors that are adequate to protect public health.

necessary dose-response calculations. The BMDS dichotomous multi-stage cancer model was run for all allowed degrees of the approximating polynomial, with a benchmark risk (BMR) of 5 percent. Instead of (q_1*) the software calculates benchmark doses (BMDs) and their 95% lower confidence levels (BMDLs). When multiplied by the BMR, the reciprocal of the BMDL gives a unit risk factor that is generally close in value to, and is used in place of (q_1*). For each tumor site, the model with the lowest value of AIC (Akaike's Information Criterion) was chosen, as long as its p-value for goodness-of-fit was above 0.1 and the absolute value of the scaled residual for the dose near the BMD was less than 2.0. The optimal model typically resulted from fitting a polynomial of 1 or 2 degrees, and the models with the lowest AIC also had the highest p-values (signifying the best fit to the data).

Interspecies extrapolation from experimental animals to humans was based on body weights (*bw*) raised to three-quarters power (US EPA, 2005; Anderson *et al.*, 1983), which for BMDLs, may be expressed in terms of body weight raised to one-quarter power, as follows:

$$BMDL_{(Human)} = BMDL_{(Animal)}\ x \left(\frac{bw_{(Animal)}}{bw_{(Human)}}\right)^{1/4}$$

The above equation is presumed to account for the toxicokinetic and toxicodynamic differences between species. Toxicokinetic modeling can sometimes eliminate the need for toxicokinetic scaling between animals and humans. This would be the case, for example, if the dose metric used in the analysis was the AUC of a directly carcinogenic metabolite. The remaining toxicodynamic differences would then be addressed, according to OEHHA practice, by scaling according to the one-eighth power of the body weight ratio.[12] Using the rate of PCE metabolism as a dose metric, on the other hand, does not account for the toxicokinetics of other downstream biological processes that determine tissue concentrations of the relevant carcinogenic species. In this case, the full cross-species scaling factor is used (US EPA, 1992).

Since PCE induced tumors at multiple sites in male mice (JISHA study) and male rats (NTP study), the combined cancer potency was also estimated for these groups using the multi-site tumor module provided in BMDS. The BMDS procedure for summing risks over several tumor sites uses the profile likelihood method. In this method, the maximum likelihood estimates (MLEs) for the multistage model parameters (q_i) for each tumor type are added together $(i.e., \sum q_0, \sum q_1, \sum q_2)$, and the resulting model is used to determine a combined BMD. Then a confidence interval for the combined BMD is calculated by computing the desired percentile of the chi-squared distribution associated with a likelihood ratio test having one degree of freedom.

Once the organ-specific and multi-site BMDLs were obtained and scaled by body-weight, the toxicokinetic model was used to estimate the continuous 24-hour air concentration that would produce the same daily metabolized dose for an adult human (i.e., the human equivalent concentration or "HEC"). The cancer potency values were then calculated by dividing the BMR of 0.05 by the HEC. Table 5 provides the calculated BMDs, BMDLs, and the interspecies-adjusted BMDLs for individual and combined tumor sites. Potency values

[12] US EPA risk assessment guidelines (2005) suggest "retaining some of the cross-species scaling factor (e.g., using the square root of the cross-species scaling factor)," when toxicokinetic modeling is used without toxicodynamic modeling.

derived from the primary studies are presented in Table 6 as unit risks factors (URFs) with units of reciprocal µg/m^3.

Inhalation Potency Value for PCE

The updated carcinogenic potency value for PCE is based on the following observations and rationale:

- Tissue-specific URF values calculated from the JISHA study are of similar magnitude to the corresponding URFs obtained from the NTP study, though somewhat lower. For mouse liver tumors, the ratio of the JISHA URF to the NTP URF was about 0.8 in both females and males. For rat MCL the corresponding ratios were 0.4 for females and 0.6 for males. The smaller URF values from the JISHA data may be due in part to the higher precision obtained by the study having used lower doses and an additional dose group.
- In both studies, the males of both species appeared to be more sensitive than the corresponding females to the tumorigenic effects of PCE.
- The URF values from both studies ranged from 2.8E-06 to 1.6E-05 (per µg/m^3), within a factor of 6. (The compared values included the multi-tumor risks for male NTP rats and male JISHA mice, as well as tissue-specific risks for other organs in mice and rats of both sexes.) Looking only at males of each species, the URFs range from 4.0E-06 to 1.6E-05.
- The highest URF was obtained from the combined site (i.e., multi-tumor) risk in male rats in the NTP study. This value was obtained by including MCL, brain, testicular, and renal tumors in the multi-tumor calculation.
- The URF values for mouse liver tumors and rat MCL were judged by OEHHA to be more certain in view of the qualitative and quantitative agreement between the two primary studies; mouse liver tumors were also found in the NCI (1977) oral exposure study.
- The unique tumors seen in the NTP study, including kidney tumors, are important to consider. The kidney is one site where the GST-pathway may contribute substantially to the cancer potency. Moreover, there is reasonable evidence that the GST-pathway may also contribute to tumorigenesis in other organ systems.
- Although it appears likely that PCE exposure increased the rate of testicular tumors in rats, the relatively high risk value obtained for testicular tumors in NTP rats may be more uncertain, given the high tumor incidence seen in the control group (71%).

Considering the above points, and also that the set of calculated values is clustered in a narrow range, the geometric mean of the male mouse and rat URFs from both studies was chosen as the best estimate of PCE cancer potency. Specifically, the geometric mean was calculated using the URF values shown in Table 7. The resulting URF, when rounded to two significant figures, is 6.1E-06 (µg/m^3)$^{-1}$. A cancer potency factor of 2.1E-02 (mg/kg-day)$^{-1}$ was also calculated from the URF using an adult body weight of 70 kg and an inspiration rate of 20 (m^3/day).

10. COMPARISON WITH U.S. EPA (2012) URF for PCE

In this section we briefly compare US EPA's 2012 URF to the OEHHA value, indicating the primary methodological differences that have resulted in differing estimates of cancer potency. The URF developed by US EPA (2012a) for inhalation exposure to PCE is 2.6E-07 $(\mu g/m^3)^{-1}$. This value is approximately 23 times less potent than OEHHA's URF, or about 20 times smaller based on US EPA's rounded URF of 3E-07 $(\mu g/m^3)^{-1}$.

The main sources of this difference are:

- US EPA used oxidation-only liver metabolism (metabolized dose) to calculate internal doses relevant to male mouse liver tumors. OEHHA used the total metabolized dose, consisting of PCE oxidation plus conjugation, in its calculations. The impact of this difference can be seen by comparing US EPA's URF, 2.6E-07 $(\mu g/m^3)^{-1}$, to OEHHA's URF for liver tumors in JISHA (1993) male mice: 3.5E-06 $(\mu g/m^3)^{-1}$ (see Table 6). OEHHA's mouse liver URF is about 13 times larger than US EPA's value. As already discussed, using total metabolism versus total oxidative metabolism (i.e., oxidation in liver, kidney and lung) is responsible for a factor of about 11 difference in the two URFs. An additional factor of roughly 1.2 is due mainly to the fact that US EPA used oxidation in liver only.
- US EPA used male mouse liver tumor data from the JISHA (1993) study as the most representative tumor-type for estimating cancer risk in humans; OEHHA used multiple tumor types in male mice and rats and both the JISHA (1993) and NTP (1986) studies, and we calculated multi-site risks for JISHA mice and NTP rats. OEHHA used a mid-range value (geometric mean) of URFs based upon all elevated tumor-types found in mice and rats in both studies. Had we followed US EPA by using only male mouse data from JISHA (1993), OEHHA's URF would have been 3.5E-06 $(\mu g/m^3)^{-1}$. Thus, using the larger body of tumor data from both studies is responsible for a factor of about 1.7 difference between the OEHHA and US EPA URFs.

Finally, it is interesting to note that US EPA (2012a) evaluated the consistency of its animal-based URF with exposure-response data for humans reported in a study that modeled increased laryngeal cancer in PCE-exposed workers (van Wijngaarden and Hertz-Picciotto, 2004). While cautioning that the human exposure information used in the exercise was subject to bias, US EPA estimated a range of URFs of 2E-06 to 8E-06 $(\mu g/m^3)^{-1}$. Although these values should be viewed as having increased uncertainty, they show greater consistency with OEHHA's URF than with US EPA's URF.

Table 5: BMDS Modeling Results for the Primary Studies

Study	Sex	Tumor Type	P-value for multi-stage model fit	Scaled residual for dose near the BMD	BMD (mg/kg-day)	BMDL (mg/kg-day)	Animal BW (kg)	BW-Scaled BMDL (mg/kg-day)
Results from Mouse Studies								
JISHA	M	Hepatocellular adenoma or carcinoma	0.22	1.17	3.06	2.16	0.048	0.350
		Harderian gland	0.99	-0.06	38.56	12.34	0.048	1.997
		Hemangioma or Hemangiosarcoma	0.35	0.94	26.61	12.98	0.048	2.100
		Combined site			2.73	1.85	0.048	0.300
	F	Hepatocellular adenoma or carcinoma	0.77	-0.23	10.33	3.84	0.035	0.574
NTP	M	Hepatocellular adenoma or carcinoma	0.85	0.03	2.46	1.79	0.037	0.272
	F	Hepatocellular adenoma or carcinoma	0.82	0.05	11.27	3.15	0.025	0.432
Results from Rat Studies								
JISHA	M	Mononuclear cell leukemia	0.79	0.07	1.34	0.89	0.45	0.251
	F	Mononuclear cell leukemia	0.37	1.05	3.99	1.84	0.30	0.472
NTP	M	Mononuclear cell leukemia	0.23	-0.31	0.92	0.51	0.44	0.144
		Testicular interstitial cell	0.35	-0.26	1.06	0.48	0.44	0.136
		Renal adenoma or carcinoma	0.93	0.07	6.76	3.24	0.44	0.913
		Brain glioma	0.15	0.62	9.45	5.07	0.44	1.426
		Combined site			0.46	0.28	0.44	0.078
	F	Mononuclear cell leukemia	0.25	-0.30	1.24	0.72	0.32	0.188

Table 6: Unit Risk Factors from Primary Studies					
Study	**Sex**	**Tumor Type**	**BW-Scaled BMDL (mg/kg-day)**	**HEC based on PBPK Model (ppm)**	**Unit Risk Factor (URF) per µg/m^3**
Results from Mouse Studies					
JISHA	M	Hepatocellular adenoma or carcinoma	0.350	2.14	3.5E-06
		Harderian gland	1.997	12.20	6.0E-07
		Hemangioma or Hemangiosarcoma	2.100	12.83	5.7E-07
		Combined site	0.300	1.83	4.0E-06
	F	Hepatocellular adenoma or carcinoma	0.574	3.51	2.1E-06
NTP	M	Hepatocellular adenoma or carcinoma	0.272	1.66	4.4E-06
	F	Hepatocellular adenoma or carcinoma	0.432	2.64	2.8E-06
Results from Rat Studies					
JISHA	M	Mononuclear cell leukemia	0.251	1.53	4.8E-06
	F	Mononuclear cell leukemia	0.472	2.88	2.6E-06
NTP	M	Mononuclear cell leukemia	0.144	0.88	8.4E-06
		Testicular interstitial cell	0.136	0.83	8.9E-06
		Renal adenoma or carcinoma	0.913	5.57	1.3E-06
		Brain glioma	1.426	8.71	8.5E-07
		Combined site	0.078	0.47	1.6E-05
	F	Mononuclear cell leukemia	0.188	1.15	6.4E-06

Table 7: URFs Used to Calculate Mean		
Species	**Study**	**URF** $(\mu g/m^3)^{-1}$
Male Mouse	JISHA (Multiple tumor)	4.02E-06
	NTP (Liver)	4.44E-06
Male Rat	JISHA (MCL)	4.81E-06
	NTP (Multiple tumor)	1.57E-05
	Geometric Mean	6.06E-06

11. REFERENCES

Anders MW, Lash L, Dekant W, Elfarra AA, Dohn DR, Reed DJ. 1988. Biosynthesis and biotransformation of glutathione-S-conjugates to toxic metabolites. CRC Critical Reviews in Toxicology 18:311-341.

Anderson EL. 1983. Quantitative Approaches in Use to Assess Cancer Risk. Risk Analysis 3:277-295.

ARB. 2012. California Environmental Protection Agency, Air Resources Board, Air Toxic Emissions Inventory, 2012.

Birner G, Richling C, Henschler D, Anders MW, Dekant W. 1994. Metabolism of tetrachloroethene in rats: identification of N epsilon-(dichloroacetyl)-L-lysine and N epsilon-(trichloroacetyl)-L-lysine as protein adducts. Chemical Research in Toxicology 7:724-732.

Birner G, Rutkowska A, Dekant W. 1996. N-acetyl-S-(1,2,2-trichlorovinyl)-L-cysteine and 2,2,2-trichloroethanol: Two novel metabolites of tetrachloroethene in humans after occupational exposure. Drug Metabolism and Disposition 24:41-48.

Bull RJ, Sasser LB, Lei XC. 2004. Interactions in the tumor-promoting activity of carbon tetrachloride, trichloroacetate, and dichloroacetate in the liver of male $B6C3F_1$ mice. Toxicology 199:169-183.

CDHS. 1991. California Department of Health Services. Health Effects of Tetrachloroethylene (PCE). Berkeley, CA.

Chiu WA, Ginsberg GL. 2011. Development and evaluation of a harmonized physiologically based pharmacokinetic (PBPK) model for perchloroethylene toxicokinetics in mice, rats, and humans. Toxicology and Applied Pharmacology 253:203-234.

Clewell HJ, Gentry PR, Kester JE, Andersen ME. 2005. Evaluation of physiologically based pharmacokinetic models in risk assessment: an example with perchloroethylene. Critical Reviews in Toxicology 35:413-433.

Dallas CE, Chen XM, O'Barr K, Muralidhara S, Varkonyi P, Bruckner JV. 1994. Development of a physiologically based pharmacokinetic model for perchloroethylene using tissue concentration-time data. Toxicology and Applied Pharmacology 128:50-59.

DeAngelo A B, Daniel FB, Wong DM, George MH. 2008. The induction of hepatocellular neoplasia by trichloroacetic acid administered in the drinking water of the male $B6C3F_1$ mouse. Journal of Toxicology and Environmental Health A71:1056-1068.

Dekant W. 1986. Metabolic conversion of tri- and tetrachloroethylene: formation and deactivation of genotoxic intermediates. Developments in Toxicology & Environmental Science 12:211-221.

Dekant W, Birner G, Werner M, Parker J, 1998. Glutathione conjugation of perchloroethene in subcellular fractions from rodent and human liver and kidney. Chemico-Biological Interactions 116: 31-43.

Dekant W, Martens G, Vamvakas S, Metzler M, Henschler D. 1987. Bioactivation of tetrachloroethylene: role of glutathione S-transferase-catalyzed conjugation versus Cytochrome P-450-dependent phospholipid alkylation. Drug Metabolism and Disposition 15:702-709.

Dekant W, Metzler M, Henschler D. 1986. Identification of S-1,2,2-trichlorovinyl-N-acetylcysteine as a urinary metabolite of tetrachloroethylene: bioactivation through glutathione conjugation as a possible explanation of its nephrocarcinogenicity. Journal of Biochemical Toxicology 1:57-72.

DeMarini DM, Perry E, Shelton ML. 1994. Dichloroacetic acid and related compounds: induction of prophage in E. coli and mutagenicity and mutation spectra in Salmonella TA100. Mutagenesis 9:429-437.

Dow. 2008. The Dow Chemical Company. Product Safety Assessment, Perchloroethylene. June 24, 2008.

Emara AM, Abo El-Noor MM, Hassan NA, Wagih AA. 2010. Immunotoxicity and hematotoxicity induced by tetrachloroethylene in Egyptian dry cleaning workers. Inhalation Toxicology 22:117-124.

Fernandez J, Guberan E, Caperos J. 1976. Experimental human exposures to tetrachloroethylene vapor and elimination in breath after inhalation. American Industrial Hygiene Association Journal 37:143-150.

Frantz SW, Watanabe PG. 1983. Tetrachloroethylene: balance and tissue distribution in male Sprague-Dawley rats by drinking-water administration. Toxicology and Applied Pharmacology 69:66-72.

Ginsberg G, Smolenski S, Hattis D, Guyton KZ, Johns DO, Sonawane B. 2009. Genetic Polymorphism in Glutathione Transferases (GST): Population distribution of GSTM1, T1, and P1 conjugating activity. Journal of Toxicology and Environmental Health, Part B.12:389-439.

Green T, Dow J, Ellis MK, Foster JR, Odum J. 1997. The role of glutathione conjugation in the development of kidney tumours in rats exposed to trichloroethylene. Chemico-Biological Interactions 105:99-117.

Green T, Odum J, Nash JA, Foster JR. 1990. Perchloroethylene-induced rat kidney tumors: an investigation of the mechanisms involved and their relevance to humans. Toxicology and Applied Pharmacology 103:77-89.

Guyton KZ, Chiu WA, Bateson TF, Jinot J, Scott CS, Brown RC, Caldwell JC. 2009. A reexamination of the PPAR-alpha activation mode of action as a basis for assessing human cancer risks of environmental contaminants. Environmental Health Perspectives 117:1664-1672.

Guyton KZ, Hogan KA, Scott CS, Cooper GS, Bale AS, Kopylev L, Barone S Jr, Makris SL, Glenn B, Subramaniam RP, Gwinn MR, Dzubow RC, Chiu WA. 2014. Human health effects of tetrachloroethylene: key findings and scientific issues. Environmental Health Perspectives 122:325-334.

Hannon-Fletcher MP, Barnett YA. 2008. Lymphocyte cytochrome P450 expression: inducibility studies in male Wistar rats. British Journal of Biomedical Science 65:1-6.

Hinchman CA, Ballatori N. 1994. Glutathione conjugation and conversion to mercapturic acids can occur as an intrahepatic process. Journal of Toxicology and Environmental Health 41:387-409.

HSDB. 2010. Hazardous Substance Data Bank. National Library of Medicine, Bethesda MD. (Internet version accessed in 2015).

IARC. 1990. International Agency for Research on Cancer. Pathology of Tumors in Laboratory Animals, 1: Tumours of the Rat. IARC Scientific Publication, No. 99, 2nd edition, Lyon France.

IARC. 2014. International Agency for Research on Cancer. Trichloroethylene, tetrachloroethylene, and some other chlorinated agents / IARC Working Group on the Evaluation of Carcinogenic Risks to Humans (2012: Lyon, France). IARC monographs on the evaluation of carcinogenic risks to humans. Vol 106.

Ikeda M, Koizumi A, Watanabe T, Endo A, Sato K. 1980. Cytogenetic and cytokinetic investigations on lymphocytes from workers occupationally exposed to tetrachloroethylene. Toxicology Letters 5: 251-256.

Irving RM, Elfarra AA. 2012. Role of reactive metabolites in the circulation in extrahepatic toxicity. Expert Opinion on Drug Metabolism & Toxicology 8:1157-1172.

Irving RM, Elfarra AA. 2013. Mutagenicity of the cysteine S-conjugate sulfoxides of trichloroethylene and tetrachloroethylene in the Ames test. Toxicology 306:157-161.

Ito Y, Yamanoshita O, Asaeda N, Tagawa Y, Lee CH, Aoyama T, Ichihara G, Furuhashi K, Kamijima M, Gonzalez FJ, Nakajima T. 2007. Di(2-ethylhexyl)phthalate induces hepatic tumorigenesis through a peroxisome proliferator-activated receptor alpha-independent pathway. Journal of Occupational Health 49:172-182.

JISHA. 1993. Japan Industrial Safety and Health Association, Japan Bioassay Research Center. Carcinogenicity study of tetrachloroethylene by inhalation in rats and mice. 2445 Hirasawa, Hadano, Kanagawa, 257-0015, Japan. March 31, 1993.

Kim S, Kim D, Pollack GM, Collins LB, Rusyn I. 2009. Pharmacokinetic analysis of trichloroethylene metabolism in male $B6C3F_1$ mice: Formation and disposition of trichloroacetic acid, dichloroacetic acid, S-(1,2-dichlorovinyl)glutathione and S-(1,2-dichlorovinyl)-L-cysteine. Toxicology and Applied Pharmacology 238:90-9.

King-Herbert, Thayer. 2006. NTP workshop: Animal model for the NTP rodent cancer bioassay: strain and stock - should we switch? Toxicologic Pathology 34: 802-805.

Klaunig JE, Babich MA, Baetcke KP, Cook JC, Corton JC, David RM, DeLuca JG, Lai DY, McKee RH, Peters JM, Roberts RA, Fenner-Crisp PA. 2003. PPAR-alpha agonist-induced rodent tumors: Modes of action and human relevance. Critical Reviews in Toxicology 33:655-780.

Kline SA, McCoy EC, Rosenkranz HS, Van Duuren BL. 1982. Mutagenicity of chloroalkene epoxides in bacterial systems. Mutation Research 101:115-125.

Kroneld R. 1987. Effect of volatile halocarbons on lymphocytes and cells of the urinary tract. Bulletin of Environmental Contamination and Toxicology 38:856-861.

Lash LH, Lipscomb JC, Putt DA, Parker JC. 1999. Glutathione conjugation of trichloroethylene in human liver and kidney: kinetics and individual variation. Drug Metabolism and Disposition 27:351-359.

Lash LH, Parker JC. 2001. Hepatic and renal toxicities associated with perchloroethylene. Pharmacological Reviews 53:177-208.

Lash LH, Putt DA, Parker JC. 2006. Metabolism and tissue distribution of orally administered trichloroethylene in male and female rats: identification of glutathione- and cytochrome P450-derived metabolites in liver, kidney, blood and urine. Journal of Toxicology and Environmental Health, Part A 69:1285-1309.

Lash LH, Putt DA, Huang P, Hueni SE, Parker JC. 2007. Modulation of hepatic and renal metabolism and toxicity of trichloroethylene and perchloroethylene by alterations in status of cytochrome P450 and glutathione. Toxicology 235:11-26.

Lash LH, Qian W, Putt DA, Desai K, Elfarra AA, Sicuri AR, Parker JC. 1998. Glutathione conjugation of perchloroethylene in rats and mice in vitro: sex-, species-, and tissue-dependent differences. Toxicology and Applied Pharmacology. 150:49-57.

Lehman-McKeeman, LD. 2010. Alpha-2u-globulin nephropathy, in McQueen CA, Comprehensive Toxicology. 2nd ed. / Oxford: Elsevier, 2010.

Liao A, Broeg K, Fox T, Tan SF, Watters R, Shah MV, Zhang LQ, Li Y, Ryland L, Yang J, Aliaga C, Dewey A, Rogers A, Loughran K, Hirsch L, Jarbadan NR, Baab KT, Liao J, Wang HG, Kester M, Desai D, Amin S, *et al.* 2011. Therapeutic efficacy of FTY720 in a rat model of NK-cell leukemia. Blood 118:2793-2800.

Marth E. 1987. Metabolic changes following oral exposure to tetrachloroethylene in subtoxic concentrations. Archives of Toxicology 60:293-299.

Mazzullo M, Grilli S, Lattanzi G, Prodi G, Turina MP, Colacci A. 1987. Evidence of DNA binding activity of perchloroethylene. Research Communications in Chemical Pathology & Pharmacology 58:215-235.

McDougal JN, Jepson GW, Clewell, Gargas ML, Andersen ME. 1990. Dermal absorption of organic chemical vapors in rats and humans. Fundamental and Applied Toxicology.14:299-308.

MDEP. 2014. Massachusettes Department of Environmental Protection, Office of Research and Standards, Tetrachloroethylene (Perchloroethylene), Inhalation Unit Risk Value, June 25, 2014.

Moyer AM, Salavaggione OE, Hebbring SJ, Moon I, Hildebrandt MA, Eckloff BW, Schaid DJ, Wieben ED, Weinshilboum RM. 2007. Glutathione S-transferase T1 and M1: gene sequence variation and functional genomics. Clinical Cancer Research. 13:7207-16.

NCI. 1977. National Cancer Institute. Bioassay of tetrachloroethylene for possible carcinogenicity. Bethesda, MD: National Institutes of Health. Report no. NCI-CGTR-13; DHEW Publication No. (NIH) 77-813.

NRC. 2010. National Research Council. Review of the Environmental Protection Agency's draft IRIS assessment of tetrachloroethylene. National Academies Press, Washington D.C.

NTP. 1986. National Toxicology Program, U.S. Department of Health and Human Services. Toxicology and carcinogenesis studies of tetrachloroethylene (perchloroethylene) (CAS no. 127-18-4) in F344/N rats and B6C3F1 mice (inhalation studies). Research Triangle Park, NC. NTP Report no. TR 311.

NTP. 2014. National Toxicology Program, U.S. Department of Health and Human Services. National Institutes of Health. 13th Report on Carcinogens. October 2, 2014.

Odum J, Green T, Foster JR, Hext PM. 1988. The role of trichloroacetic acid and peroxisome proliferation in the differences in carcinogenicity of perchloroethylene in the mouse and rat. Toxicology and Applied Pharmacology 92:103-112.

OEHHA. 1992. Office of Environmental Health Hazard Assessment. Health Effects of Perchloroethylene. May 1992.

OEHHA. 2001. Office of Environmental Health Hazard Assessment. Public Health Goal for Tetrachloroethylene in Drinking Water. August 2001.

OEHHA. 2009. Office of Environmental Health Hazard Assessment. Technical Support Document for Cancer Potency Factors. May 2009.

OEHHA. 2012. Office of Environmental Health Hazard Assessment. Technical Support Document for Exposure Assessment and Stochastic Analysis. August 2012.

Ohtsuki T, Sato K, Koizumi A, Kumai M, Ikeda M. 1983. Limited capacity of humans to metabolize tetrachloroethylene. International Archives of Occupational and Environmental Health 51:381-90.

Reddy MB,Yang RS, Andersen ME, Clewell HJ. 2005. Physiologically-based pharmacokinetic modeling: science and applications. Wiley-Interscience, Hoboken, NJ.

Riihimaki V, Pfaffli P. 1978. Percutaneous absorption of solvent vapors in man. Scandinavian Journal of Work and Environmental Health. 4:73-85.

Rooseboom M, Vermeulen NP, Groot EJ, Commandeur JN. 2002. Tissue distribution of cytosolic beta-elimination reactions of selenocysteine Se-conjugates in rat and human. Chemico-Biological Interactions. 140:243-264.

Seiji K, Jin C, Watanabe T, Nakatsuka H, Ikeda M. 1990. Sister chromatid exchanges in peripheral lymphocytes of workers exposed to benzene, trichloroethylene, or tetrachloroethylene, with reference to smoking habits. International Archives of Occupational and Environmental Health. 62:171-176.

Schreiber JS, Hudnell HK, Geller AM, House DE, Aldous KM, Force MS, Langguth K, Prohonic EJ, Parker JC, 2002. Apartment residents' and day care workers' exposures to tetrachloroethylene and deficits in visual contrast sensitivity. Environmental Health Perspectives. 110:655-664.

Sokol L, Loughran TP, Jr. 2006. Large granular lymphocyte leukemia. Oncologist 11:263-273.

Thomas J, Haseman JK, Goodman JI, Ward JM, Loughran TP, Jr., Spencer PJ. 2007. A review of large granular lymphocytic leukemia in Fischer 344 rats as an initial step toward evaluating the implication of the endpoint to human cancer risk assessment. Toxicological Sciences 99:3-19.

Tiruppathi C, Miyamoto Y, Ganapathy V, Roesel RA, Whitford GM, Leibach FH. 1990. Hydrolysis and transport of proline-containing peptides in renal brush-border membrane vesicles from dipeptidyl peptidase IV-positive and dipeptidyl peptidase IV-negative rat strains. Jounal of Biological Chemistry 265:1476-83.

Toraason M, Butler MA, Ruder A, Forrester C, Taylor L, Ashley DL, Mathias P, Marlow KL, Cheever KL, Krieg E, Wey H. 2003. Effect of perchloroethylene, smoking, and race on oxidative DNA damage in female dry cleaners. Mutation Research/Genetic Toxicology and Environmental Mutagenesis 539:9-18.

Tucker JD, Sorensen KJ, Ruder AM, McKernan LT, Forrester CL, Butler MA. 2011. Cytogenetic analysis of an exposed-referent study: perchloroethylene-exposed dry cleaners compared to unexposed laundry workers. Environmental Health 10:16.

USEPA. 1991. Alpha-2u-globulin: Association with chemically induced renal toxicity and neoplasia in the male rat. Washington, DC: U.S. Environmental Protection Agency, National Center for Environmental Assessment. Report no. EPA/625/3-91/019F.

USEPA. 1992. Draft report: A cross-species scaling factor for carcinogen risk assessment based on equivalence of mg/kg(3/4)/day. Federal Register 57:24151-24173.

USEPA. 2005. U.S. Environmental Protection Agency. Guidelines for carcinogen risk assessment. Risk Assessment Forum. Report no. EPA/630/P-03/001F.

US EPA. 2011. U.S. Environmental Protection Agency. Toxicological Review of Trichloroacetic Acid, In Support of Summary Information on the Integrated Risk Information System (IRIS), Report no. EPA/635/R-09/003F.

US EPA. 2012a. U.S. Environmental Protection Agency. Toxicological Review of Tetrachloroethylene (Perchloroethylene), In Support of Summary Information on the Integrated Risk Information System (IRIS). Report no. EPA/635/R-08/011F.

US EPA. 2012b. U.S. Environmental Protection Agency. Integrated Risk Information System (IRIS) Chemical Assessment Summary: Tetrachloroethylene (Perchloroethylene).

US EPA. 2012c. U.S. Environmental Protection Agency. Lymphohematopoietic Cancers Induced by Chemicals and Other Agents: Overview and Implications for Risk Assessment, EPA/600/R-10/095F.

US EPA. 2015. U.S. Environmental Protection Agency, National Center for Environmental Assessment. Benchmark Dose Software (BMDS) Version 2.6.0.1.

Vamvakas S, Dekant W, Berthold K, Schmidt S, Wild D, Henshler D. 1987. Enzymatic transformation of mercapturic acids derived from halogenated alkenes to reactive and mutagenic intermediates. Biochemical Pharmacology 36:2741-2748.

Vamvakas S, Dekant W, Henschler D. 1989a. Genotoxicity of haloalkene and haloalkane glutathione S-conjugates in porcine kidney cells. Toxicology *in Vitro* 3:151-156.

Vamvakas S, Herkenhoff M, Dekant W and Henschler D. 1989b. Mutagenicity of tetrachloroethene in the Ames test—metabolic activation by conjugation with glutathione. Journal of Biochemical Toxicology. 4:21–27.

Van Duuren BL, Kline SA, Melchionne S, Seidman I. 1983. Chemical structure and carcinogenicity relationships of some chloroalkene oxides and their parent olefins. Cancer Research. 43:159-162.

van Wijngaarden E, Hertz-Picciotto I. 2004. A simple approach to performing quantitative cancer risk assessment using published results from occupational epidemiology studies. Science of the Total Environment. 332:81-7.

Vlaanderen J, Straif K, Ruder A, Blair A, Hansen J, Lynge E, Charbotel B, Loomis D, Kauppinen T, Kyyronen P, Pukkala E, Weiderpass E, Guha N. 2014. Tetrachloroethylene exposure and bladder cancer risk: a meta-analysis of dry-cleaning-worker studies. Environmental Health Perspectives. 122:661-666.

Volkel W, Friedewald M, Lederer E, Pahler A, Parker J, Dekant W, 1998. Biotransformation of perchloroethene: dose-dependent excretion of trichloroacetic acid, dichloroacetic acid, and N-acetyl-S-(trichlorovinyl)-L-cysteine in rats and humans after inhalation. Toxicology and Applied Pharmacology. 153:20-27.

Walles SA. 1986. Induction of single-strand breaks in DNA of mice by trichloroethylene and tetrachloroethylene. Toxicology Letters 31:31-35.

Wang JL, Chen WL, Tsai SY, Sung PY, Huang RN. 2001. An *in vitro* model for evaluation of vaporous toxicity of trichloroethylene and tetrachloroethylene to CHO-K1 cells. Chemico-Biological Interactions 137:139-154.

Wheeler JB, Stourman NV, Their R, Dommermuth A, Vuilleumier S, Rose JA, Armstrong RN, Guengerich, FP, 2001. Conjugation of haloalkanes by bacterial and mammalian glutathione transferases: mono- and dihalomethanes. Chemical Research in Toxicology 14:1118-1127.

White IN, Razvi N, Gibbs AH, Davies AM, Manno M, Zaccaro C, De Matteis F, Pahler A, Dekant W. 2001. Neoantigen formation and clastogenic action of HCFC-123 and perchloroethylene in human MCL-5 cells. Toxicology Letters 124:129-138.

Yang Q, Ito S, Gonzalez FJ. 2007. Hepatocyte-restricted constitutive activation of PPAR alpha induces hepatoproliferation but not hepatocarcinogenesis. Carcinogenesis 28:1171-1177.

Yoo HS, Bradford BU, Kosyk O, Shymonyak S, Uehara T, Collins LB, Bodnar WM, Ball LM, Gold A, Rusyn I. 2015. Comparative analysis of the relationship between trichloroethylene metabolism and tissue-specific toxicity among inbred mouse strains: liver effects. Journal of Toxicology and Environmental Health A. 78:15-31.

Yoshioka T, Krauser JA, Guengerich FP. 2002. Tetrachloroethylene oxide: hydrolytic products and reactions with phosphate and lysine. Chemical Research in Toxicology 15:1096-1105.

APPENDIX A

PBPK Model Code for Simplified, Inhalation-Only Adaptation of Chiu and Ginsberg (2011) PCE Model, for Mice, Rats, and Humans (Written in Berkeley Madonna)

{ Inhalation-Only Adaptation of Chiu and Ginsberg (2010) PCE Model for MICE }

```
METHOD RK4
STARTTIME = 0
STOPTIME=504
DT = 0.002

ppm=10      {inhaled conc in ppm}
CInh=If (Mod(Time,24)<=6 AND Mod(Time,168)<=120) Then (ppm*165.83/24450) Else 0

; BW=0.037 {NTP Male}
; BW=0.048 {JISHA Male}
; BW=0.025 {NTP Female}
  BW=0.035 {JISHA Female}

QC=11.6*BW^0.75
QP=QC*2.5*exp(0.325015)
QM=QP/0.7   {minute volume, L/h}
DResp=QP*exp(0.203)
; Intake=QM*Cinh*24/BW

QGut=0.141*QC
QLiv=0.02*QC
QKid=0.091*QC
QFat=0.07*QC
QRap=0.461*QC
QSlw=0.217*QC

PB=18.6
PResp=79.1/PB
PGut=62.1/PB
PLiv=48.8/PB
PKid=79.1/PB
PRap=62.1/PB
PSlw=79.1/PB
PFat=1510.8/PB

VResp=0.0007*BW
VRespEff=VResp*PResp*PB
VRespLum=0.004667*BW
VGut=0.049*BW
VLiv=0.055*BW
VKid=0.017*BW
VRap=0.1*BW
VFat=0.07*BW
VBld=0.049*BW
VSlw=(0.8897*BW)-(VResp+VGut+VLiv+VKid+VRap+VFat+VBld)

{ Metabolic Constant Calculations }
{=================================}
KMo=                88.6
lnKMC=              -5.35885
ClCo=               1.57
lnClC=              3.18103
lnKM2C=             15
lnCl2OxC=           -1.20051
KmKidLivo=          0.616
```

```
ClKidLivo=          0.0211
VMaxLungLivo=       0.07
VMaxTCVGo=          35.3
lnVMaxTCVGC=        10.2
ClTCVGo=            0.656
lnClTCVGC=          -9.17006
VMaxKidLivTCVGo=    0.15
ClKidLivTCVGo=      0.24

KM=KMo*exp(lnKMC)
VMax= KM*ClCo*VLiv*exp(lnClC)

KM2=KM*exp(lnKM2C)
VMax2=KM2*(VMax/KM)*exp(lnCl2OxC)

KMKid=KM*KMKidLivo
VMaxKid=(VMax/KM)*KMKid*(VKid/VLiv)*ClKidLivo

KMClara=KM*PLiv/(PB*PResp)
VMaxClara=VMax*VMaxLungLivo

VMaxTCVG=VMaxTCVGo*VLiv*exp(lnVMaxTCVGC)
KmTCVG=VMaxTCVG/(ClTCVGo*exp(lnClTCVGC))

VMaxKidTCVG=VMaxTCVG*(VKid/VLiv)*VMaxKidLivTCVGo
KmKidTCVG=VMaxKidTCVG/(ClKidLivTCVGo*(VKid/VLiv)*(VMaxTCVG/KMTCVG))
{==================================}

Init AGut=0             Limit AGut>=0
Init AResp=0            Limit AResp>=0
Init AExhResp=0         Limit AExhResp>=0
Init AInhResp=0         Limit AInhResp>=0
Init ALiv=0             Limit ALiv>=0
Init AKid=0             Limit AKid>=0
Init ARap=0             Limit ARap>=0
Init ASlw=0             Limit ASlw>=0
Init AFat=0             Limit AFat>=0
Init ABld=0             Limit ABld>=0

{Respiratory Model Concentrations}
CInhResp=AInhResp/VRespLum          {conc resp lumen during inh, mg/L}
CResp=AResp/VRespEff                {conc resp tract tissue, mg/L}
CExhResp=AExhResp/VRespLum          {conc resp lumen during exh, mg/L}

{Blood Concentrations}
CVGut=(AGut/VGut)*(1/PGut)
CVLiv=(ALiv/VLiv)*(1/PLiv)
CVKid=(AKid/VKid)*(1/PKid)
CVRap=(ARap/VRap)*(1/PRap)
CVSlw=(ASlw/VSlw)*(1/PSlw)
CVFat=(AFat/VFat)*(1/PFat)
CVBld=(ABld/VBld)
CArt=(QC*CVBld+QP*CInhResp)/(QC+(QP/PB))

{Metabolism: P450 Oxidation}
RAMetLng=(VMaxClara*CResp)/(KMClara+CResp)
RAMetLiv1=(VMax*CVLiv)/(KM+CVLiv)+(VMax2/KM2)*CVLiv
RAMetKid1=(VMaxKid*CVKid)/(KMKid+CVKid)
```

```
{Metabolism: GST Conjugation}
RAMetLiv2=(VMaxTCVG*CVLiv)/(KMTCVG+CVLiv)
RAMetKid2=(VMaxKidTCVG*CVKid)/(KMKidTCVG+CVKid)

{Respiratory Model Mass Balance Equations}
AInhResp'=QM*CInh+DResp*(CResp-CInhResp)-QM*CInhResp
AResp'=DResp*(CInhResp+CExhResp-2*CResp)-RAMetLng
AExhResp'=QM*(CInhResp-CExhResp)+QP*((CArt/PB)-CInhResp)+DResp*(CResp-CExhResp)

{Other Mass Balance Equations}
AGut'=QGut*(CArt-CVGut)
ALiv'=(QLiv*CArt)+(QGut*CVgut)-((QLiv+QGut)*CVLiv)-RAMetLiv1-RAMetLiv2
AKid'=QKid*(CArt-CVKid)-RAMetKid1-RAMetKid2
ARap'=Qrap*(CArt-CVRap)
ASlw'=QSlw*(CArt-CVSlw)
AFat'=QFat*(CArt-CVFat)
ABld'=(QFat*CVFat)+((QGut+QLiv)*CVLiv)+(QSlw*CVSlw)+(QRap*CVRap)+(QKid*CVKid)-
(QC*CVBld)

init MetCum=0           Limit MetCum>=0
init LivOxCum=0         Limit LivOxCum>=0

MetTot=RAMetLng+RAMetLiv1+RAMetKid1+RAMetLiv2+RAMetKid2
MetCum'=If TIME>=336 Then (MetTot/(7*BW)) Else 0
LivOxCum'=If TIME>=336 Then (RAMetLiv1/(7*BW)) Else 0
```

{ Inhalation-Only Adaptation of Chiu and Ginsberg (2011) PCE Model for RATS }

```
METHOD RK4
STARTTIME = 0
STOPTIME=504
DT = 0.002

ppm=50      {inhaled conc in ppm}
CInh=If (Mod(Time,24)<=6 AND Mod(Time,168)<=120) Then (ppm*165.83/24450) Else 0

; BW=0.44   {NTP Male}
  BW=0.45   {JISHA Male}
; BW=0.32   {NTP Female}
; BW=0.30   {JISHA Female}

QC=13.3*BW^0.75
QP=QC*1.9*0.61643
QM=QP/0.7   {minute volume, L/h}
DResp=QP*exp(1)
; Intake=QM*Cinh*24/BW

QGut=0.153*QC
QLiv=0.021*QC
QKid=0.141*QC
QFat=0.07*QC
QRap=0.279*QC
QSlw=0.336*QC

PB=15.1
PResp=32.7/PB
PGut=40.6/PB
PLiv=50.3/PB
PKid=32.7/PB
PRap=40.4/PB
PSlw=21.6/PB
PFat=1489.3/PB

VResp=0.0005*BW
VRespEff=VResp*PResp*PB
VRespLum=0.004667*BW
VGut=0.032*BW
VLiv=0.034*BW
VKid=0.007*BW
VRap=0.088*BW
VFat=0.07*BW
VBld=0.074*BW
VSlw=(0.8995*BW)-(VResp+VGut+VLiv+VKid+VRap+VFat+VBld)

{ Metabolic Constant Calculations }
{=================================}
KMo=              69.7
lnKMC=            -0.805889
ClCo=             0.36
lnClC=            2.02965
KMKidLivo=        1.53
ClKidLivo=        0.0085
VMaxLungLivo=     0.0144
```

```
VmaxTCVGo=        93.9
lnVMaxTCVGC=      10.2
ClTCVGo=          2.218
lnClTCVGC=        -6.99311
VMaxKidLivTCVGo=  0.15
ClKidLivTCVGo=    0.098

KM=KMo*exp(lnKMC)
VMax=KM*ClCo*VLiv*exp(lnClC)

KMKid=KM*KMKidLivo
VMaxKid=(VMax/KM)*KMKid*(VKid/VLiv)*ClKidLivo

KMClara=KM*PLiv/(PB*PResp)
VMaxClara=VMax*VMaxLungLivo

VMaxTCVG=VMaxTCVGo*VLiv*exp(lnVMaxTCVGC)
KmTCVG=VMaxTCVG/(ClTCVGo*exp(lnClTCVGC))

VMaxKidTCVG=VMaxTCVG*(VKid/VLiv)*VMaxKidLivTCVGo
KmKidTCVG=VMaxKidTCVG/(ClKidLivTCVGo*(VKid/VLiv)*(VMaxTCVG/KMTCVG))
{================================}

Init AGut=0             Limit AGut>=0
Init AResp=0            Limit AResp>=0
Init AExhResp=0         Limit AExhResp>=0
Init AInhResp=0         Limit AInhResp>=0
Init ALiv=0             Limit ALiv>=0
Init AKid=0             Limit AKid>=0
Init ARap=0             Limit ARap>=0
Init ASlw=0             Limit ASlw>=0
Init AFat=0             Limit AFat>=0
Init ABld=0             Limit ABld>=0

{Respiratory Model Concentrations}
CInhResp=AInhResp/VRespLum    {conc resp lumen during inh, mg/L}
CResp=AResp/VRespEff          {conc resp tract tissue, mg/L}
CExhResp=AExhResp/VRespLum    {conc resp lumen during exh, mg/L}


{Blood Concentrations}
CVGut=(AGut/VGut)*(1/PGut)
CVLiv=(ALiv/VLiv)*(1/PLiv)
CVKid=(AKid/VKid)*(1/PKid)
CVRap=(ARap/VRap)*(1/PRap)
CVSlw=(ASlw/VSlw)*(1/PSlw)
CVFat=(AFat/VFat)*(1/PFat)
CVBld=(ABld/VBld)
CArt=(QC*CVBld+QP*CInhResp)/(QC+(QP/PB))

{Metabolism: P450 Oxidation}
RAMetLiv1=(VMax*CVLiv)/(KM+CVLiv)
RAMetKid1=(VMaxKid*CVKid)/(KMKid+CVKid)
RAMetLng=(VMaxClara*CResp)/(KMClara+CResp)

{Metabolism: GST Conjugation}
RAMetLiv2=(VMaxTCVG*CVLiv)/(KMTCVG+CVLiv)
RAMetKid2=(VMaxKidTCVG*CVKid)/(KMKidTCVG+CVKid)
```

```
{Respiratory Model Mass Balance Equations}
AInhResp'=QM*CInh+DResp*(CResp-CInhResp)-QM*CInhResp
AResp'=DResp*(CInhResp+CExhResp-2*CResp)-RAMetLng
AExhResp'=QM*(CInhResp-CExhResp)+QP*((CArt/PB)-CInhResp)+DResp*(CResp-CExhResp)

{Other Mass Balance Equations}
AGut'=QGut*(CArt-CVGut)
ALiv'=(QLiv*CArt)+(QGut*CVgut)-((QLiv+QGut)*CVLiv)-RAMetLiv1-RAMetLiv2
AKid'=QKid*(CArt-CVKid)-RAMetKid1-RAMetKid2
ARap'=Qrap*(CArt-CVRap)
ASlw'=QSlw*(CArt-CVSlw)
AFat'=QFat*(CArt-CVFat)
ABld'=(QFat*CVFat)+((QGut+QLiv)*CVLiv)+(QSlw*CVSlw)+(QRap*CVRap)+(QKid*CVKid)-
(QC*CVBld)

init MetCum=0     Limit MetCum>=0

MetTot=RAMetLng+RAMetLiv1+RAMetKid1+RAMetLiv2+RAMetKid2
MetCum'=If TIME>=336 Then (MetTot/(7*BW)) Else 0
```

{ Inhalation-Only Adaptation of Chiu and Ginsberg (2011) PCE Model for HUMANS }

```
METHOD RK4
STARTTIME=0
STOPTIME=840
DT = 0.0002

ppm=10      {inhaled conc in ppm}
CInh=ppm*165.83/24450

BW=70
QC=16*BW^0.75
QP=0.96*1.28*QC
QM=QP/0.7   {minute volume, L/h}
DResp=QP*exp(-5.06)
; Intake=QM*Cinh

QGut=0.19*QC
QLiv=0.065*QC
QKid=0.19*QC
QFat=0.05*QC
QRap=0.285*QC
QSlw=0.22*QC

PB=14.7
PResp=58.6/PB
PGut=59.9/PB
PLiv=61.1/PB
PKid=58.6/PB
PRap=59.9/PB
PSlw=70.5/PB
PFat=1450/PB

VResp=0.00018*BW
VRespEff=VResp*PResp*PB
VRespLum=0.002386*BW
VGut=0.02*BW
VLiv=0.025*BW
VKid=0.0043*BW
VRap=0.088*BW
VFat=0.199*BW
VBld=0.077*BW
VSlw=(0.8560*BW)-(VResp+VGut+VLiv+VKid+VRap+VFat+VBld)

{ Metabolic Constant Calculations }
{=================================}
KMo=              55.8
lnKMC=            6.9
ClCo=             0.202
lnClC=            0.2501
KMKidLivo=        1.04
ClKidLivo=        0.0125
lnClKidLivC=      4.57452
VMaxLungLivo=     0.0128
VMaxTCVGo=        0.665
lnVMaxTCVGC=      10.2
ClTCVGo=          0.0196
```

```
lnClTCVGC=        5.59162
VMaxKidLivTCVGo=  0.15
ClKidLivTCVGo=    0.14

KM=KMo*exp(lnKMC)
VMax=KM*ClCo*VLiv*exp(lnClC)

KMKid=KM*KMKidLivo
VMaxKid=(VMax/KM)*KMKid*(VKid/VLiv)*ClKidLivo*exp(lnClKidLivC)

KMClara=KM*PLiv/(PB*PResp)
VMaxClara=VMax*VMaxLungLivo

VMaxTCVG=VMaxTCVGo*VLiv*exp(lnVMaxTCVGC)
KmTCVG=VMaxTCVG/(ClTCVGo*exp(lnClTCVGC))

VMaxKidTCVG=VMaxTCVG*(VKid/VLiv)*VMaxKidLivTCVGo
KmKidTCVG=VMaxKidTCVG/(ClKidLivTCVGo*(VKid/VLiv)*(VMaxTCVG/KMTCVG))
{================================}

{Metabolism: P450 Oxidation}
RAMetLiv1=(Vmax*CVLiv)/(KM+CVLiv)
RAMetKid1=(VMaxKid*CVKid)/(KMKid+CVKid)
RAMetLng=(VMaxClara*CResp)/(KMClara+CResp)

{Metabolism: GST Conjugation}
RAMetLiv2=(VMaxTCVG*CVLiv)/(KMTCVG+CVLiv)
RAMetKid2=(VMaxKidTCVG*CVKid)/(KMKidTCVG+CVKid)

Init AGut=0             Limit AGut>=0
Init AResp=0            Limit AResp>=0
Init AExhResp=0         Limit AExhResp>=0
Init AInhResp=0         Limit AInhResp>=0
Init ALiv=0             Limit ALiv>=0
Init AKid=0             Limit AKid>=0
Init ARap=0             Limit ARap>=0
Init ASlw=0             Limit ASlw>=0
Init AFat=0             Limit AFat>=0
Init ABld=0             Limit ABld>=0

{Respiratory Model Concentrations}
CInhResp=AInhResp/VRespLum    {conc resp lumen during inh, mg/L}
CResp=AResp/VRespEff          {conc resp tract tissue, mg/L}
CExhResp=AExhResp/VRespLum    {conc resp lumen during exh, mg/L}

{Blood Concentrations}
CVGut=(AGut/VGut)*(1/PGut)
CVLiv=(ALiv/VLiv)*(1/PLiv)
CVKid=(AKid/VKid)*(1/PKid)
CVRap=(ARap/VRap)*(1/PRap)
CVSlw=(ASlw/VSlw)*(1/PSlw)
CVFat=(AFat/VFat)*(1/PFat)
CVBld=(ABld/VBld)
CArt=(QC*CVBld+QP*CInhResp)/(QC+(QP/PB))  {arterial blood conc}

{Respiratory Model Mass Balance Equations}
AInhResp'=QM*CInh+DResp*(CResp-CInhResp)-QM*CInhResp
AResp'=DResp*(CInhResp+CExhResp-2*CResp)-RAMetLng
AExhResp'=QM*(CInhResp-CExhResp)+QP*((CArt/PB)-
```

```
CInhResp)+DResp*(CResp-CExhResp)

{Other Mass Balance Equations}
AGut'=QGut*(CArt-CVGut)
ALiv'=(QLiv*CArt)+(QGut*CVgut)-((QLiv+QGut)*CVLiv)-RAMetLiv1-RAMetLiv2
AKid'=QKid*(CArt-CVKid)-RAMetKid1-RAMetKid2
ARap'=Qrap*(CArt-CVRap)
ASlw'=QSlw*(CArt-CVSlw)
AFat'=QFat*(CArt-CVFat)
ABld'=(QFat*CVFat)+((QGut+QLiv)*CVLiv)+(QSlw*CVSlw)+(QRap*CVRap)+(QKid*CVKid)-
(QC*CVBld)

MetTot=(RAMetLng+RAMetLiv1+RAMetKid1+RAMetLiv2+RAMetKid2)*(24/BW)
```

APPENDIX B

Dose Metric Values used in Dose-Response Modeling Obtained from PBPK Inhalation Model

PBPK Estimated Total Metabolized Doses
(mg/kg-day)

JISHA Mouse (Male and female weights: 0.048 and 0.035 kg)		
Exposure Concentration (ppm)	**Male**	**Female**
10	5.10	5.22
50	18.15	18.44
250	72.73	73.94
JISHA Rat (Male and female weights: 0.45 and 0.30 kg)		
Exposure Concentration (ppm)	**Male**	**Female**
50	1.82	1.88
200	6.47	6.67
600	15.32	15.83
NTP Mouse (Male and female weights: 0.037 and 0.025 kg)		
Exposure Concentration (ppm)	**Male**	**Female**
100	32.78	33.38
200	60.25	61.40
NTP Rat (Male and female weights: 0.44 and 0.32 kg,		
Exposure Concentration (ppm)	**Male**	**Female**
200	6.48	6.63
400	11.38	11.66